High-Resolution Infrared Spectroscopy of Weakly Bound Molecular Complexes

DAVID J. NESBITT*

Department of Chemistry and Biochemistry, University of Colorado, and Joint Institute for Laboratory Astrophysics, National Bureau of Standards and University of Colorado, Boulder, Colorado 80309

Received December 1, 1987 (Revised Manuscript Received April 18, 1988)

Contents

I.	Introduction	843
II.	Experimental Methods	844
	A. Equilibrium Cell Methods	845
	B. Supersonic Molecular Beam Methods	846
III.	Molecular Systems	847
	A. Homogeneous Complexes	847
	1. $(HF)_n$	847
	2. $(HCl)_n$	849
	3. $(HCCH)_n$	849
	4. $(CO_2)_n$	850
	5. $(N_2O)_n$	851
	6. $(HCN)_n$	851
	7. $(NH_3)_n$	852
	B. Heterogeneous Complexes	853
	1. H_2–M Complexes	853
	2. Hydrogen Halide–Inert Gas Complexes	855
	3. HF–Diatomic and HF–Triatomic Complexes	858
	4. HF–Hydrocarbon Complexes	860
	5. HCN–Hydrogen Halide Complexes	860
	6. Polyatomic–Inert Gas Complexes	862
IV.	Discussion	863
	A. Vibrational Predissociation/Relaxation Dynamics	863
	B. Intermolecular Bend–Stretch Coupling	865
	C. Equilibrium and Vibrationally Averaged Structures	866
V.	Summary	867

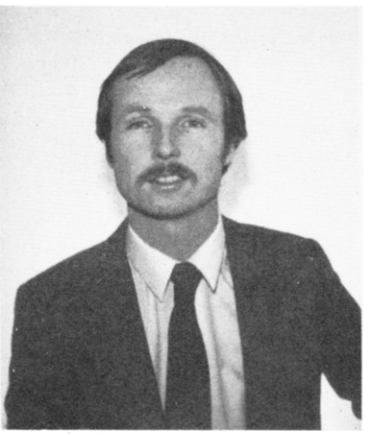

David J. Nesbitt did his undergraduate studies in physics and chemistry at Harvard University, spending a year (1973–1974) working with Prof. J. Peter Toennies at the Max Planck Institute for Stroemungsforschung in Goettingen, West Germany. He then taught secondary school science and math for 2 years at Colorado Academy in Denver, prior to entering a Ph.D. program in chemical physics at the University of Colorado, Boulder. His thesis work was divided between the theory of liquid-phase reaction dynamics and experimental laser-initiated photochemical kinetics, for which he was presented the Nobel Laureate Signature Award by the American Chemical Society. Dr. Nesbitt was awarded a Miller Fellowship for Basic Research at the University of California, Berkeley, where he developed methods for high-sensitivity tunable IR detection of ions and radicals. At present Dr. Nesbitt is a Fellow of the Joint Institute for Laboratory Astrophysics (National Bureau of Standards and University of Colorado), a Physicist with NBS Boulder Labs, and Associate Professor Adjoint in the Department of Chemistry at the University of Colorado. His experimental research there has involved application of direct absorption IR laser techniques to study of radical kinetics and nonlinear vibrational dynamics of jet-cooled molecules.

I. Introduction

The study of the weak attractions[1,2] between molecules is fundamental to an enormous variety of chemical and physical phenomena, including inelastic energy transfer,[3–5] photofragmentation dynamics,[6] line broadening,[7] theories of hydrogen bonding,[8] and transition between gas and condensed phases.[9] Such widespread relevance has served to catalyze considerable research effort toward elucidating the full potential energy surfaces that govern these weak but centrally important intermolecular forces. One of the most direct and sensitive probes of the topology of these surfaces has been high-resolution rotational, vibrational, and electronic spectroscopy to characterize the bound states of these weakly associated molecules. Indeed, the impressive power of methods based on high-resolution microwave[10,11] and laser-induced fluorescence[12] (LIF) spectroscopy for probing rotational and electronic degrees of freedom has been largely responsible for developing our intuitions concerning structure and dynamics in weakly bound systems. With few exceptions,[13,14] however, the microwave studies have been limited to *ground vibrational* states of complexes and hence probe primarily the near-equilibrium regions of the potential surface. Nonetheless, tremendous insight into the local topology near the minimum has been inferred via averaging of electrical multipolar properties of the monomers over wide amplitude motion in the low-frequency intermolecular modes. Given favorable Franck–Condon factors, electronic spectroscopy[12,15] of molecular complexes has proven quite a powerful probe of *vibrationally excited* states of molecular complexes. In fact, much of theoretical interest in vibrational predissociation[16] dynamics of complexes stems from the early studies of $I_2(v)$–M (M = rare gas) in electronically

*Staff Member, Quantum Physics Division, National Bureau of Standards.

0009-2665/88/0788-0843$06.50/0

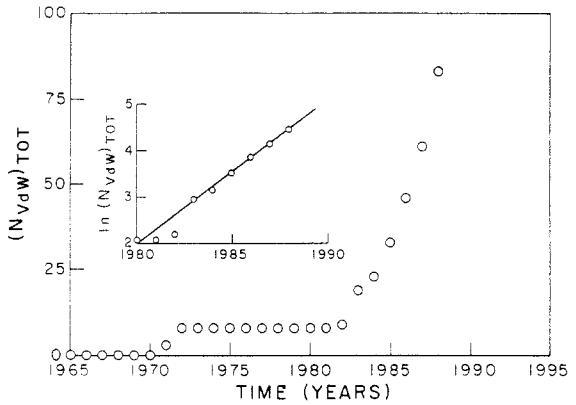

Figure 1. Plot of the total number of rotationally resolved and assigned spectra of vibrationally excited complexes as a function of year since 1965. The value for 1988 includes all of the papers in press or communicated to the author in preprint form. The explosive growth since the early 1980s is shown in a semilogarithmic plot (insert). The linear fit to the data suggests a doubling of the total number of species investigated every 2.1 years!

excited states.[12,15,17] These studies, unfortunately, do not provide much information on vibrationally excited regions of the potential surface for the *ground electronic* state,[18] and yet it is precisely this part of the potential that controls both long- and short-range collisional dynamics of the monomers.

High-resolution infrared spectroscopy of molecular complexes in principle contains much detailed information on these regions of the intermolecular potential surface, but has proven more difficult to implement due to insensitive detection methods, lack of tunable high-resolution infrared optical probes, etc. In recent years, however, several methods for high-resolution infrared spectroscopy of weakly bound complexes have been developed that have triggered a virtual explosion of new spectroscopic data (see Figure 1); it is toward a systematic review of these methods and recent results that this paper is directed. Ten years ago there would have been little material for such a review, and yet, given the present pace of research efforts, the task of a comparable review in a few years is daunting. By way of example, Figure 1 displays a plot of the total number of rotationally resolved and assigned vibrational spectra of molecular complexes as a function of year. The precipitous increase in this output from 1983 to present is nearly exponential, with a doubling time of approximately 2.1 years! The time seems therefore ripe for a summary of these early, rapidly developing, and very exciting efforts.

At the outset it is useful to delineate the boundaries of this review. (1) The focus will be limited primarily to experimental studies, although the inclusion of some theoretical efforts will be both appropriate and necessary. As this entire issue of *Chemical Reviews* is dedicated to van der Waals molecules, the reader is referred to other articles for more involved theoretical discussions. (2) Simply as a matter of practicality the experimental work treated in this review will be restricted to IR methods of sufficient resolution to achieve both rotational-state resolution and spectroscopic assignment. This admittedly somewhat arbitrary criterion will exclude from detailed discussion much of the interesting and provocative OPO, CO_2, and the early rotationally unresolved F-center laser vibrational predissociation studies by several groups.[19-27] Fortunately much of this material has been discussed recently by Miller.[28] This criterion will also exclude the more recent spectrally resolved but rotationally unassigned data on ethylene dimer.[29,30] However, these restrictions offer the advantage of focusing the discussion on systems where a more unambiguous analysis, interpretation, and comparison between different sets of experimental data are possible. Nonetheless, we shall see that even with high-resolution, rotationally resolved data, there is still entirely sufficient room for controversial interpretation of the experimental results.

The organization of this review will be as follows. As the major advancements in the field have been largely spurred by new ultrasensitive detection schemes in the IR, a brief discussion of these methods is presented in section II. In section III, the research on each of the molecular complexes successfully analyzed via high-resolution IR spectroscopy is summarized. Given the roughly 80 different complexes, isotopomers, vibrational states, etc. covered in this review, quick reference data for each of these classes of molecules are provided in tabular form. The enormous breadth of molecular systems notwithstanding, these studies highlight several common themes, which are discussed in section IV. Section V presents a brief, and hopefully not too myopic, summary and outlook on some important questions to be addressed in the next generation of experiments, the results of which might be the starting point of a future review at a further stage of the field's development.

II. Experimental Methods

Though the availability of high-resolution infrared data on complexes represents a relatively recent breakthrough, much of the first spectroscopic evidence for the existence of weakly bound molecular clusters was obtained in the infrared, through the observation of excess absorption in gas mixtures that could not be observed in either gas individually.[31-39] It is a little surprising, therefore, that high-resolution refinements of the earliest of these IR studies did not take place for four decades, and not until much of the pioneering work had already been established in the microwave (rotational) and visible/UV (electronic) regions of the spectrum. The reason for such a time lag was not lack of scientific interest but rather a lack of appropriate high-resolution sources of IR light[40] as well as a lack of adequately sensitive detection methods. This situation has changed dramatically in recent years. In this section the various high- and moderate-resolution methods are briefly summarized.

The various experimental techniques that have developed for high-resolution IR spectroscopy of complexes rely on two fundamentally different schemes for detecting the interaction of light with molecules. Stated most simply, the two strategies are (1) to measure the influence of light on the molecules or (2) to measure the influence of molecules on the light. Examples of the former are laser-induced fluorescence,[12,15,17,18] photoacoustic,[41] molecular beam electric resonance,[10] and optothermal[28,42] spectroscopies. Examples of the latter are direct absorption,[32-39] intracavity laser resonance,[43] and Fourier transform[11] spectroscopies. A further distinction between these various methods depends on the method of "synthesis" of the molecular complexes, i.e.,

cooled equilibrium gas cells, or much lower temperature (albeit nonequilibrium) molecular beams formed by supersonic jet expansions.

A. Equilibrium Cell Methods

The methods exploited for infrared detection of weakly bound complexes in an equilibrium cell have relied on classic Beer's law or Fourier transform IR spectroscopies, both of which are essentially direct absorption techniques. The rather considerable demands for sensitivity in direct absorption can be readily appreciated by the following simple calculation for a triatomic van der Waals complex comprised of A and BC. If one makes the simplifying assumption that the rotational and vibrational degrees of freedom of BC remain unaffected in the complex, the equilibrium constant for formation of A–BC in a typical quantum state can be shown to be[44]

$$K(T) = \left[\frac{h^2\mu_{A\text{-}BC}}{2\pi kT\mu_{BC}m_A}\right]^{3/2} e^{D_0/kT} \qquad (2.1)$$

where D_0 is the dissociation energy of the van der Waals bond and $\mu_{A\text{-}BC}$ and μ_{BC} are reduced masses. Since the rotational degrees of freedom of BC are often strongly quenched by complexation, eq 2.1 represents only an approximation to the equilibrium constant per populated quantum state. To consider a specific example, for D_0 = 100 cm^{-1} and masses 40, 1, and 19 amu for A, B, and C, respectively, roughly 1 in 10^9 of the molecules will be complexed in a typical quantum state for 1 Torr of A and BC at room temperature. For a complex with a strong, Doppler-limited absorption cross section in the near-IR,[45] one predicts absorptions on the order of a few parts per million per meter of path length! This is within the limits of shot noise limited direct absorption methods,[46] but these often require high-frequency modulation of the absorbing species to avoid the low-frequency accumulation of technical noise in the IR light source and detectors, i.e., methods that are difficult to implement in a static cell.

One can greatly enhance these weak absorptions by operation at reduced temperatures, higher sample pressures, or enhanced path lengths obtainable with White cell, multiple-pass optics. For the specific case of 1 Torr of BC in 10 Torr of A, the concentration of A–BC complexes in a typical quantum state can be estimated to be 7×10^9 complexes/cm^3 in a cell cooled to 210 K. In a 100-m White cell, this concentration would yield on the order of 10% absorption of the incident light for near-IR Doppler-broadened line widths, provided that the light source is spectrally narrow with respect to these widths. One outstanding problem, however, is that the BC molecule (by assumption a strong IR absorber) is present in roughly a billion-fold excess, which, in addition to absorption from $(BC)_n$ complexes as well, can render portions of the desired spectrum optically black.

The experimental difficulties associated with strongly absorbing excess monomer species, however, can be finessed elegantly for complexes of nonabsorbing monomer constituents, as in the early studies of complexes of H_2.[47-52] Since only the complexes can exhibit a dipole-allowed IR spectrum in the H_2 stretching region, one can choose to operate at relatively high cell pressures and cooled cell temperatures to shift the equilibrium toward higher concentration of H_2 complexes. One difficulty with such an approach is the limit of pressure broadening on spectral resolution, though by virtue of the large rotational constants of these H_2-containing complexes, fully resolved rotational structure could be detected and analyzed.[50-57]

Direct absorption spectroscopy in an equilibrium cell for systems where IR-absorbing monomers are present in great excess requires a much higher resolution probe such as permitted by microwave oscillators[13,14,58] or CW single-frequency infrared[40] lasers and, preferably, subunits with a sparse absorption spectrum. Pine has successfully developed a scheme of nonlinear difference frequency mixing of a dye and Ar^+ laser that can generate tunable, narrow-band (<1 MHz) IR light from 2.2–4.2 μm at the few microwatt power level.[40,59] In conjunction with a long-path, cooled White cell, this weak but spectrally bright source of light has permitted high-resolution study of species such as hydrogen halide dimers and inert gas–hydrogen halide complexes.[60-65] The equilibrium distributions in the cooled cell have also facilitated thermodynamic study of the absolute binding energies in these complexes.[62] Bevan and coworkers[66-69] have similarly utilized a commercial tunable F-center laser by either sequential mode hop (300 MHz) or higher resolution ($\lesssim$2 MHz)[70] scanning of the output frequency. Diode lasers have also been used in long-path absorption cells for study of hydrogen halide dimers,[71] despite the considerable difficulty in tuning these lasers over large regions of the infrared spectrum. The lack of ability to "modulate" the absorbers, however, forces the detection bandwidth essentially near DC, where several sources of $1/f$ noise (e.g., fluctuations in the laser light amplitude) can, in principle, limit sensitivity. More typically, however, spectral congestion due to absorption from thermally populated rovibrational states of monomers and undesired complexes limits the sensitivity of these equilibrium methods.

Cooled White cell techniques have been extended into regions of the spectrum less convenient for tunable IR lasers by use of interferometric, Fourier transform methods.[72-82] The limiting resolution of an FTIR instrument scales as the length traveled by the interferometric mirrors and consequently cannot begin to challenge the $>10^2$-m coherence lengths routinely achievable by frequency-stabilized CW lasers. However, for Doppler-limited, pressure- or predissociation-broadened spectra lines, this limitation of FTIR methods may not be important. Two correspondingly powerful advantages of the Fourier transform approach are (1) the entire spectrum is obtained for all frequencies at once, which enhances considerably the duty cycle for data collection per spectrally resolvable frequency element, and (2) by virtue of the heterodyne nature of FT methods, the desired absorption information is encoded in a detection bandwidth well removed from the excess noise contributions near DC. In conjunction with a long-path White cell, these relatively high-resolution FTIR techniques have been used to investigate many of the inter- and intramolecular vibrational modes in more strongly bound complexes such as HCN dimer,[80] HCN–HF,[73-78] and HF dimer.[81,82]

One attractive feature of these equilibrium methods for forming and studying molecular complexes is that

relative populations of various quantum states are independently and simply determined by equilibrium statistical mechanics. From analysis of the spectral line intensities and intensity ratios therefore, one can deduce thermodynamic properties[62,64,65] and vibrational term values[13,14] for the complex. Additionally, at the relatively warm temperatures required to prevent freezing out of the subunits, hot-band sequences from low-frequency modes can be observed that provide important information on *multiply*-excited vibrational states. A particularly elegant use of these cell methods has been to probe rotational states populated near the dissociation limit and to extract precise bond dissociation energies for rare gas–hydrogen halide complexes.[64,65] In spite of the considerable difficulties, therefore, with thermal congestion in cooled-cell spectra, these equilibrium methods are a rich source of information for highly rovibrationally excited states of molecules near dissociation.

B. Supersonic Molecular Beam Methods

IR spectroscopy of weakly bound complexes in a supersonically cooled molecular beam[12,28,83,84] has several advantages and disadvantages. On the one hand, very efficient formation of the complexes is favored by the low translational temperatures in the jet. Indeed, this method of "synthesis" has served valiantly for LIF,[12,15,17,18,84] molecular beam electric resonance (MBER),[85–97] and FT microwave studies[98–104] of numerous complexes. Furthermore, the spectroscopy of the complexed species can be greatly simplified by the corresponding low rotational and, to a lesser extent, vibrational temperatures in the jet. Additionally, the compression of the Boltzmann distribution into a smaller number of quantum states implies greater detection sensitivity per complex, as well as the virtually complete elimination of spectral congestion from internally excited rotational and vibrational states of the monomer. Finally, angular collimation of the molecular beams can be exploited to achieve much higher frequency resolution than permitted by Doppler and pressure broadening in a cooled cell.

Balancing these advantages is a simple fact. Although a significant fraction of the molecules can be complexed, the total number density of complexes is still quite small, decreases rapidly with distance downstream from the expansion orifice, and under typical conditions offers only relatively short path lengths for interaction with the light source. Consequently, only methods with high sensitivities are viable candidates; several are briefly described below.

One of the first methods for IR spectroscopy of complexes was based on pulsed laser vibrational excitation of complexes in a skimmed molecular beam.[19,20,22,23,105–108] Vibrational predissociation of these complexes leads to a depletion of cluster signals monitored with an electron bombardment mass spectrometer. The extent of fragmentation of the complex upon electron bombardment, however, is not well-known;[109] a given mass signal, therefore, may arise from predissociation of higher molecular weight clusters and preclude unambiguous assignment of spectra in the absence of detailed isotopic substitution tests[110] or rotational resolution.[23]

Highly sensitive, high-resolution IR laser spectroscopy in molecular beams can be achieved via bolometric detection of small changes in the thermal energy content of the beam.[26,28,42,111–120] This "optothermal" technique, developed initially by Scoles and co-workers,[111] relies on a highly collimated CW molecular beam that is crossed with a chopped CW IR laser. If excited complexes predissociate away from the beam over the flight path to the bolometer, a modulated depletion synchronous with the chopping frequency is observed. Nonpredissociating molecules excited by the laser exhibit an *increase* in the thermal energy of the beam while predissociating molecules exhibit a *decrease*; this proves to be an important advantage in assigning complex spectra with contributions from monomer and cluster species. The high degree of collimation over the length of the flight path permits sub-Doppler resolution (a few MHz), which in turn permits detailed study of excess line broadening attributable to vibrational predissociation or intramolecular relaxation. Since the magnitude of the depletion signal scales linearly with IR laser power, this method offers the greatest sensitivity for relatively high-power lasers and hence has been extensively used with line-tunable CO_2 lasers, wave guide CO_2 lasers, and high-resolution F-center lasers.

Direct absorption laser spectroscopy in supersonic jets, whereby one simply monitors attenuation in power of a laser crossing a molecular beam, has proven to be a surprisingly sensitive method for investigating weakly bound molecular complexes. Unlike the bolometric methods, however, the high sensitivity does not require a moderately powerful light source. In a light absorpton measurement the ultimate S/N will be limited by quantum shot noise on the photon arrival rate. Even for IR laser power levels of a few microwatts, this shot noise translates into fractional absorption sensitivities of better than $10^{-6}/\mathrm{Hz}^{1/2}$, which makes IR spectroscopy of complexes feasible for a much broader range of weak but tunable lasers such as diode lasers and CW nonlinear frequency generation schemes. Hayman et al.[121] obtained the first direct absorption, infrared diode laser spectrum of complexes in a pulsed pinhole expansion. Achievement of these levels of sensitivity requires careful control of technical laser amplitude noise. The short time duration of the absorption signal during the gas pulse was exploited to discriminate against low-frequency amplitude noise in the diode laser source. Multiple passage of the IR light through the relatively short absorption path length of a pinhole expansion source can improve detection sensitivity by as much as an order of magnitude and has made feasible the study of several complexes.[121–124]

Dramatic enhancement in the sensitivity of these direct absorption laser methods is available via reshaping of the expansion geometry. Lovejoy et al.[125–130] have developed methods for IR spectroscopy of complexes in one-dimensional "slit" expansions,[131] whereby single-pass absorption path lengths of up to 4 cm are obtained. White cell optics can further enhance this path length to over 50 cm in only 2 cm of downstream flow. The hydrodynamics of the slit expansion also collapses the velocity distribution along the slit, thus narrowing Doppler widths to $\lesssim$40–100 MHz, depending on the mass of the expansion gas. Since this narrowing is not obtained by skimming molecules from the beam, peak absorption strengths can be commensurately in-

creased by up to an order of magnitude. In conjunction with careful subtraction methods to reduce laser amplitude fluctuations to near shot noise levels, detection sensitivities of better than 10^8 molecules/cm^3 per quantum state can be obtained. One very important aspect of the slit expansion geometry is that the molecular densities decrease only as 1/distance downstream. This translates into more efficient clustering at lower stagnation pressures and the ability to "tune" the rovibrational temperature of the complexes (roughly 5–30 K). This permits study of thermally excited, low-frequency vibrations in clusters and, most importantly, helps bridge the gap between pinhole (typically $T_{rot} < 1$–2 K) and cooled-cell ($T_{rot} > 100$ K) conditions.

Nonlinear coherent antistokes Raman spectroscopy (CARS) in supersonic jets[132–134] has been used by Nibler and co-workers to investigate the rovibrational structure of complexes at moderate ($\sim$0.1 cm^{-1}) resolution. Though not nearly as sensitive as the bolometric or direct absorption infrared methods, it uniquely permits investigation of IR-forbidden, Raman-active modes in a complex. Additionally, simply by tuning the frequency separation of the two visible lasers, one can observe both high-frequency (intramolecular) modes and low-frequency (intermolecular) modes via the same laser source. Spectral resolution is limited by the bandwidth of the pulsed visible lasers, and typically rotational structure in complexes is not resolved. Nonetheless, CARS has been used to observe and model rotational band contours and thereby distinguish between different geometries postulated for a complex.[132–134]

There have been two far-infrared spectroscopic techniques developed in parallel by Klemperer and co-workers[135–138] and Saykally and co-workers[43,139–141] to investigate low-frequency intermolecular modes in complexes. A fixed-frequency, CO_2 laser pumped far-infrared (FIR) laser acts as the probe; specific transitions in the complex are brought into resonance by Stark tuning of the J and m_J levels. In the method of Klemperer and co-workers, the Stark resonance is detected by a change in beam flux through electrostatic state selectors, followed by electron bombardment mass spectrometry. This is qualitatively similar to the double-resonance technique of DeLeon and Muenter,[142] which had been previously demonstrated without Stark tuning using a tunable F-center laser. Saykally and co-workers, on the other hand, measure the intracavity depletion of the FIR laser caused by Stark tuning transitions in the complex into resonance. Analysis of the spectral data requires understanding the relative Stark tuning rates of the upper and lower states, but particularly the high sensitivity provided by nonlinear, intracavity methods looks very promising for study of many complexes. These FIR lasers have been mixed with microwave radiation to generate a tunable, high-resolution FIR laser source,[143] for use in direct absorption studies of van der Waals complexes without the complication of Stark tuning.

III. Molecular Systems

The discussion of the various molecular complexes investigated via rotationally resolved IR spectroscopic methods can be conveniently broken down into *homogeneous* and *heterogeneous* complexes, in which the molecular constituents are either identical or different, respectively.

A. Homogeneous Complexes

1. $(HF)_n$

The strength of hydrogen bonding in HF has provided the incentive for much experimental[60–62,81,82,85,86,105,108,110,117,142,144–150] and theoretical[151–158] effort on HF dimers and higher polymers. Infrared spectroscopic observation of HF dimers and polymers in the null gap region between R(0) and P(1) monomer lines was made as early as 1958 by Kuipers[144] and by Smith[145,146] using low-resolution, direct absorption methods in high-pressure cells. By monitoring the pressure dependence of the integrated absorption signals, Smith assigned three spectral features at 3856, 3895, and 3963 cm^{-1} to the dimer species and attributed them to ν_2 ("bonded" hydrogen stretch), ν_1 ("free" hydrogen stretch), and some combination band, respectively. Later higher resolution spectrophotometric efforts by Herget et al.[147] and Himes and Wiggins[148] at 0.1- and 0.03-cm^{-1} resolution, respectively, revealed partially resolved structure on the combination band, which was presumably rotational in origin. Fully rotationally resolved information on HF and DF dimers was supplied soon thereafter by molecular beam electric resonance MBER studies by Dyke et al.[85] A detailed analysis[151–153] of their radio frequency and microwave spectra indicated a highly nonrigid, hydrogen-bonded complex which executed rapid tunneling motion between the two equivalent structures, HF–HF and FH–FH. These data permitted fitting of a good-quality potential energy surface for HF dimer by Barton and Howard[153] which exhibited a slightly bent equilibrium geometry with a linear F–H–F hydrogen bond. Laser vibrational predissociation spectra of HF dimers and polymers by Lisy et al.[105] revealed three peaks assigned to the dimer species at 3720, 3878, and 3970 cm^{-1} and attributed to ν_2, ν_1, and the same combination band, respectively, as reported by Smith[145,146] and Herget et al.[147]

With the development of stabilized ($\lesssim$1 MHz) tunable difference frequency IR laser methods,[59] Pine was able to construct a spectrometer with frequency resolution limited only by Doppler and/or pressure broadening. In conjunction with cooled, long-path White cells, this direct absorption spectrometer revealed an extremely rich spectrum of HF dimer, DF dimer, and the DF–HF/HF–DF mixed dimers in the HF and DF stretching region.[60,61] The spectra exhibit fully resolved and assignable tunneling doublets, asymmetry doubling for $K = 1$ levels, extensive K subband structure, and vibrational bands for each of the two fundamental H(D) stretching frequencies. These spectra have been definitively analyzed and assigned to A ($\Delta K = 0$) and B ($\Delta K = \pm 1$) type subbands in both the "free" (ν_1) and "bonded" (ν_2) H(D) stretch (see Table I). On the basis of (i) absolute dimer absorption intensities under equilibrium conditions, (ii) dimer partition functions calculated from the spectroscopic data, and (iii) the assumption that the integrated absorption strength of HF does not change significantly upon complexation, Pine et al. calculate the absolute dissociation energy to be 1038 (+43, −34) cm^{-1},[62] significantly lower than

TABLE I. Summary of Vibrational Data for HF and DF Dimers

species	equilib geometry	ν_0/cm^{-1}	mode descrip	$(\nu - \nu_{monomer})/cm^{-1}$	$\Delta\nu_{FWHM}$/MHz	D_0/cm^{-1}	ref
HF		3961.4229					
$(HF)_2$	near linear	3930.9030 3930.4593	$\nu_1^{\pm}$ free H stretch	−30.7418	13.4	1038	60–62, 117
		3868.3127 3867.4206	$\nu_2^{\pm}$ bonded H stretch	−93.5563	410	60–62, 117	
		400.75 399.78	$\nu_6^{\pm}$ torsion				81 81
		7679	$2\nu_1$ free H stretch overtone		<5000[a]		82
		7542	$2\nu_2$ bonded H stretch overtone		<5000[a]		82
$(DF)_2$	near linear	(2882.1)[b]	$\nu_1^{\pm}$	−24.8	<41[c]		60, 61, 160
		2834.6190 2834.5499	$\nu_2^{\pm}$	−72.4			60, 61, 160

[a] Limited by residual experimental broadening. [b] Average of $K = 1 \leftarrow 0$ and $0 \leftarrow 1$ origins. [c] Limited by residual Doppler broadening in a slit jet.

previous experimental results[146,149] but in fair agreement with semiempirical[153] and ab initio[157] potential energy surface calculations.

This pioneering study of the high-frequency vibrations in HF dimer by Pine and co-workers demonstrated conclusively that IR spectra in systems at energies far above the dissociation limit could reveal extensive rovibrational structure. This was indeed a surprising observation in light of the estimate by Klemperer[158] of a predissociation lifetime in HF dimer of 50 ps, which by uncertainty broadening would have washed out most of the rotational structure and thereby seriously limited the potential power and sensitivity of these high-resolution IR methods.

The excellent agreement of combination differences with microwave data and quality of fits to the rotational analysis strongly suggest that all but one of the peaks in the earlier low-resolution IR experiments[105,145–147] correspond to an unresolved P branch in the ν_1 band and two unresolved Q band heads in the ν_2 band. The strong peak observed at 3720 cm^{-1} by Lisy et al.[105] has no corresponding absorption feature attributable to the high-resolution dimer spectrum and has more recently been assigned[110] to the HF trimer species via isotopic labeling studies. There are no studies to date that exhibit rotationally resolved structure in trimer and higher oligomers of HF.

The vibrationally averaged structure in a molecule as nonrigid as HF dimer is strongly K dependent, and therefore a rotational analysis based on a semirigid asymmetric top Hamiltonian proves necessary for each K subband. Pine et al.[61] show via a novel analysis using Padé approximant methods that the apparently anomalous pattern of K subband origins can be physically understood to arise from "rotational saturation", where the equilibrium slightly bent dimer becomes centrifugally bent into an L-shaped geometry in the limit of high-K excitation.

The predissociation line widths in HF dimer, as inferred from the homogeneous component to the absorption line shape, are dramatically vibrational mode dependent. In the original studies by Pine et al.,[60,61] predissociation broadening in the ν_2 mode was estimated to be 410 ± 60 MHz FWHM from a least-squares fit of the ν_2 $K = 1 \leftarrow 1, 0 \leftarrow 0$ spectrum. No significant excess line widths above Doppler and pressure broadening were observed for ν_1 excitation in HF dimer or in either ν_1 or ν_2 modes observed in DF dimer.[61] DeLeon and Meunter[142] utilized an infrared–microwave double-resonance MBER apparatus to establish an upper limit to predissociation widths of 30 ± 5 MHz by pumping a single line [$^rP_0^+(2)$] with an F-center laser. In a sub-Doppler bolometer study of the ν_1 mode of HF dimer by Huang et al.[117] much improved estimates of predissociation line widths in the ν_1 mode, $K = 1 \leftarrow 0$ were determined to be 13.4 ± 1 MHz (FWHM), independent of J states populated in a 2 K jet. If these excess widths can be fully attributed to predissociation, this indicates a 30-fold faster breakup of the complex when vibrationally excited at the hydrogen-bonded H stretch than in the free H stretch. This observation provided one of the first definitive examples of a nonstatistical behavior in vibrationally excited molecules and is a lesson that is repeated in many of the complexes investigated via high-resolution IR methods. The issue of inferring lifetimes directly from experimentally observed line widths is complicated and is discussed in more detail in section IV. Nonetheless, these early studies surprisingly indicated that rigorous lower limits to predissociation lifetimes in HF dimer complexes excited above the dissociation limit were well in excess of 10^4 vibrational periods of the HF stretch.

At the 210–220 K cell temperatures employed in the Pine studies,[60,61] low-frequency intermolecular vibrations are thermally excited, which lead to hot-band progressions built on each of the assigned vibrations whose analysis should provide detailed information on these modes as well. A more direct probe of these intermolecular modes has been initiated by Von Puttkamer and Quack,[81] utilizing FTIR absorption techniques at 0.02-cm^{-1} resolution in a 250–300 K White cell, in which a low-frequency mode at 400 cm^{-1} is observed and tentatively assigned to a torsional vibration. Interestingly, the analysis suggests tunneling frequencies *increase* by 1.5 with *torsional* excitation, in contrast with the roughly 3-fold *decrease* in tunneling splittings observed by Pine et al.[60,61] upon HF *stretch* excitation. An increase in the tunneling frequencies with torsional excitation would be consistent with a small component of the torsional displacements along the tunneling coordinate. Conversely, tunneling might be inhibited by excitation in an HF stretch mode, since the tunneling motion must transfer the stretching vibrational quantum between the two HF subunits. Von Puttkamer and Quack[82] have also utilized this FTIR technique to investigate the first overtone spectrum of HF dimer near 7600 cm^{-1}. The narrow spectral widths observed (on the order of 0.16 cm^{-1}) in these bands appear still to be

TABLE II. Summary of Vibrational Data for Complexes of HCl[a]

species	equilib geometry	ν_0/cm^{-1}	mode descrip	$(\nu - \nu_{monomer})$/ cm^{-1}	$\Delta\nu_{FWHM}$/ MHz	D_0/cm^{-1}	ref
HCl		2885.9758					
Ne–HCl	linear	2886.277	ν_1 HCl stretch	+0.301	<45[b]		201
		2908.802	$\nu_1 + \nu_2(\Pi)$	+22.826	<45[b]		201
		2901.9623	$\nu_1 + \nu_2(\Sigma)$	+15.9865	<45[b]		201
		2907.129	$\nu_1 + \nu_3(\Sigma)$	+21.153			
		(22.525)[d]	($\nu_2(\Pi)$)				
		(15.685)[d]	($\nu_2(\Sigma)$)				
		(20.852)[d]	($\nu_3(\Sigma)$)				
Ar–HCl	linear	2884.2087	ν_1 HCl stretch	−1.7671	<40[b]	114.7	65, 201
		2918.2624	$\nu_1 + \nu_2(\Pi)$	+32.2866	<40[b]		201
		2907.8374	$\nu_1 + \nu_2(\Sigma)$	+21.8616	<40[b]		201
		2916.8461	$\nu_1 + \nu_3$ vdW stretch	+30.8703	<40[b]		201
		33.9797	$\nu_2(\Pi)$				140
		(34.0537)[d]					
		23.6568	$\nu_2(\Sigma)$				139
		(23.6287)[d]					
		32.4358	ν_3 vdW stretch				141
		(32.6374)[d]					
$(HCl)_2$	near linear	2890.7610	ν_1^+ $K = 1 \leftarrow 0$ free H stretch	+4.7852	<45[b]	431	62, 63
		2857.2353	$\nu_2^{\pm}$ bonded H	−28.7405	<45[b]		63
		2838.8972	stretch	−47.0780			
HCN–HCl	linear	3309.0286	ν_1 HCN stretch	−2.444	c		79

[a] Data provided for the ^{35}Cl isotope. [b] Line width limited by residual Doppler broadening in a slit jet. [c] Limited by Doppler and pressure broadening in a cooled White cell. [d] Frequency quoted in parentheses is for $(\nu_1 + \nu_{vdW}) - \nu_1$ for comparison with FIR studies.

dominated by residual pressure broadening and suggest long predissociation lifetimes even at energies 7 times the dissociation limit.

2. $(HCl)_n$

As in the case of HF dimer, the first spectral evidence for HCl dimer was via low-resolution IR absorption in high-pressure, long path length cells. In these studies by Rank et al.,[33,34] three extra peaks that varied quadratically with pressure were observed in the null gap region between R(0) and P(1) of the monomer, with intensities in the natural-abundance ratios of the three isotopic forms of a complex with two Cl atoms. Partially resolved structure in the dimer spectrum attributed to rotations was later observed with a higher resolution spectrometer.[159] No studies have been reported in the microwave on HCl dimer. Consequently the extent of rotationally resolved information on HCl dimer is primarily limited to the experiments of Ohashi and Pine,[63] utilizing tunable difference frequency laser absorption in a 64–80-m path length, 130 K White cell (see Table II). Nonetheless, these studies permitted a rotational analysis of the one tunneling component of ν_1^+ and both tunneling components of $\nu_2^{\pm}$ vibration, for a range of $K'' = 0$, 1, and 2. Combination differences between $\nu_2^+ = 1 \leftarrow 0$ and $\nu_1^+ = 1 \leftarrow 0$ for the ground state were used to verify the assignments.

Tunneling between the two equivalent configurations in HCl dimer proves to be extremely facile, resulting in sums of tunneling splittings between the ground and ν_2 excited state of 18 cm^{-1}. This is significantly larger than the corresponding ground (0.66 cm^{-1}) and ν_2 excited state (0.22 cm^{-1}) values for HF dimer.[61] These splittings are apparently large with respect to the zero-point energy differences between the $H^{35}Cl$–$H^{37}Cl$ and $H^{37}Cl$–$H^{35}Cl$ conformations. Thus these two species interconvert rapidly, resulting in a spectrum characteristic of an averaged isotopic geometry, widely split by tunneling interactions, i.e., consistent with the early low-resolution observations.[33,34]

As in the HF dimer study, excess broadening above the Doppler limit was determined via Voigt line shape fitting to the spectrum. The data in the $\nu_2^{\pm}$ free H stretch bands could be adequately fit with a Lorentzian component of only 160 ± 40 MHz FWHM. This is on the order of expected pressure-broadening contributions at 4 Torr and indicates that vibrational predissociation in ν_2 excited HCl dimer occurs at least an order of magnitude more slowly than in the corresponding vibration in HF dimer. Similar investigation of the ν_1 mode indicated homogeneous line widths somewhat narrower (100–140-MHz FWHM), but again reasonably accounted for by pressure broadening. Recent slit jet studies on HCl dimer indicate a homogeneous line width less than the 45-MHz FWHM residual Doppler broadening in the jet.[160] This diminution of predissociation rate in HCl dimer and DF dimer over HF dimer is consistent with models that predict the excess energy to be distributed predominantly into rotation of the monomer fragments and is briefly addressed in section IV.

3. $(HCCH)_n$

The first IR spectroscopy of acetylene dimers was obtained by Pendley and Ewing,[39] utilizing FTIR absorption methods in a long-path White cell at 215 K. Five vibrational bands were observed, four of which could be assigned based on the electrostatic potential energy surface of Sakai et al.[161] Although no rotational structure could be resolved in these FTIR studies,[39] the band contours could be well reproduced with the slipped-parallel (i.e., adjacent but staggered) geometry predicted theoretically.[161] Higher resolution F-center spectra obtained by Miller et al.[114] exhibited six well-separated bands (labeled A–F) in the 3300-cm^{-1} region, with discrete rotational structure evident in several of the bands. No rotational assignment was presented, but the appearance of several bands prompted the suggestion that multiple conformers of acetylene dimer might exist. These results were followed up by systematic

TABLE III. Summary of Vibrational Data for Complexes Formed from Miscellaneous Polyatomic Species

species	equilib geometry	ν_0/cm^{-1}	mode descrip	$(\nu - \nu_{monomer})$/ cm^{-1}	$\Delta\nu_{FWHM}$/ MHz	ref
HCN						
$(HCN)_2$	linear	3308.3175	ν_1 free H stretch	−3.156	<1[a]	171
		3241.5588	ν_2 bonded H stretch	−69.914	26	80, 171
$(HCN)_3$	linear	3306.8025	ν_1 free H stretch	−4.671	<1[a]	171
	linear	3231.1	ν_2	−80.4	15000	171
	linear	3212.9335	ν_3	−98.540	56	171
	cyclic	3273.545	ν_1	−37.928	*b*	171
CO_2						
$(CO_2)_2$	slipped parallel	3714.011	correlates with $\nu_1 + \nu_3$ in CO_2	−0.772	<1[a]	118
$(CO_2)_3$	cyclic	3613.819			<20[b]	120
HCCH						
$(HCCH)_2$	slipped parallel	(3280)[d]			<25	162
$(HCCH)_3$	cyclic	(3265.6)[d]			*b*	124
N_2O						
$(N_2O)_2$	slipped parallel	3478.4357	correlates with $\nu_1 + \nu_3$ in N_2O	−2.3832	<1	167
Ar–N_2O	near T	2223.9078	ν_3 asym stretch	+0.1509	*c*	123
OCS						
Ne–OCS	near T	2062.3170	ν_3 asym stretch	+0.1157	*c*	121, 122
Ar–OCS	near T	2061.7404	ν_3 asym stretch	−0.4609	*c*	121, 122
Kr–OCS	near T	2061.3457	ν_3 asym stretch	−0.8556	*c*	121, 122

[a] Line width limited by residual broadening in a sub-Doppler skimmed beam. [b] Line width limited by unresolved K structure. [c] Line width limited by residual Doppler broadening in a pinhole jet. [d] Precise band origin uncertain.

pressure-dependent studies by Fischer et al.,[26] in which it was shown that significant contributions to the spectra were present for the A and B bands from species larger than dimers.

Ironically, the first rotationally resolved and assigned IR spectroscopy of acetylene complexes was not for the dimer, but rather the trimer. A reinvestigation of the B band by Prichard et al.[124] using direct absorption of an F-center laser in a pulsed jet expansion revealed a very simple progression of equally spaced lines that could be conclusively assigned to a cyclic trimer with either C_{3h} or D_{3h} symmetry (see Table III). The surprising simplicity of this trimer spectrum results from the fact that $C = B/2$ for a rigid planar molecule; provided there is sufficiently small change in the constants on vibrational excitation, the highly degenerate spectrum of this oblate top consists of many lines overlapped to within the experimental resolution. Prichard et al.[124] point out that small changes in rotational constants, nonzero inertial defects, etc. will break this exact degeneracy and therefore broaden the lines inhomogeneously. This is likely to account for the asymmetric and broadened lines that Miller et al.[114] observed in the B band but attributed to homogeneous effects.

Recently, the entire series of bands A–F has been reinvestigated at high resolution by Bryant et al.[162] using bolometer-based methods. The rotational structure in the D, E, and F bands is now assigned to acetylene dimer, for $K = 0 \leftarrow 1$, $1 \leftarrow 0$, and $2 \leftarrow 1$, respectively. The spectrum exhibits intensity alternation in adjacent ^pP and ^pR lines that indicate an equilibrium structure with 2-fold symmetry about the C axis. In addition, sequence bands for these three subbands are observed, most likely due to an unassigned, low-frequency van der Waals mode still excited in the jet. Most interestingly, an upper state K-dependent homogeneous lifetime is observed in this series; for $K' =$ 2, 1, and 0 the line widths are reported as 25.7 MHz, 19.5 MHz, and instrument limited, respectively. This trend is at least physically consistent with the centrifugal effects along the dissociation coordinate anticipated for rotation around the A axis. Bryant et al.[162] claim that the C band results from a non-slipped-parallel dimer structure and suggest that it may result in a T-shaped isomer; however, no detailed assignment of the C band is available.

4. $(CO_2)_n$

The high-resolution saga of carbon dioxide dimers and polymers is rather extensive and colorful and points nicely to the power of IR (vibrational) versus microwave (rotational) spectroscopies for studies of complexes comprised of subunits without molecular dipoles. The first analysis of CO_2 dimer was performed by Mannik et al.,[38] based on low-resolution IR spectroscopy in a cooled (192 K) long-path absorption cell. They interpreted their spectrum of the $\nu_1 + 2\nu_2$ band as an indication of a T-shaped structure for the CO_2 dimer, as would be expected from the angular dependence of a dominant quadrupole–quadrupole[9] interaction at fixed intermolecular separation.

This noncentrosymmetric interpretation was supported by dipole moment studies by Novick et al.,[87] who observed a 1% electrostatic refocusing on the mass peak associated with CO_2 dimer in a molecular beam. However, the later experimental results of Barton et al.[163] indicated no measurable refocusing on the dimer mass peak and suggested that higher polymers were influencing the Novick results.[87] From their data, Barton et al.[163] were able to place an upper limit of 10^{-2} D on the dipole moment of the dimer and argued that a T-shaped structure would exhibit an induced dipole moment of 0.25–0.32 D based on electrostatic moments and polarizability of the CO_2 subunits. Furthermore, by modeling the intermolecular potentials as electrostatic plus hard-sphere interactions, they demonstrated that although the T-shaped geometry is energetically preferred for *fixed* center of mass separations, the $1/R^5$ attractive part of the quadrupole–quadrupole potential strongly favors the *decrease* in separation accessible in a slipped-parallel configuration. When one allows intermolecular distances to vary, a second *deeper* minimum is predicted from the electrostatic model for a centrosymmetric (and hence zero dipole moment) configuration with a 3.44-Å center of mass separation of the two CO_2 units and a slippage angle of 57°.

A subsequent reanalysis of the low-resolution IR spectrum of CO_2 dimer by Kopec[164] indicated that the data could be consistent with both a T-shaped and slipped-parallel configuration. A remeasurement of the focusing properties of CO_2 dimer by Lobue et al.[165] reffirmed the original dipole moment values obtained by Novick et al.[87] In a molecular beam measurement by Gough et al.[112] the $\nu_1 + \nu_3$ and $2\nu_2 + \nu_+$ bands were studied with multimode F-center laser excitation and bolometer detection. The spectra yielded unresolved features of 2–3-cm^{-1} width whose line shapes could be fairly well reproduced with a rotational band contour calculated for the minimum energy, C_{2h} geometry of Barton et al.[163]

CARS in a free jet expansion by Nibler and coworkers[134] was used to investigate the ν_1 Raman-allowed vibration. For a slipped-parallel C_{2h} geometry, the ν_1 vibrations on each of the CO_2 subunits can couple "in phase" (A_g) and "out of phase" (B_u), only the former of which would be Raman active. By contrast, for a T-shaped C_{2v} geometry, both ν_1 vibrations would remain Raman active. The observation of a single rotationally unresolved peak in the CARS spectrum at 1285 cm^{-1} was therefore interpreted as support for a slipped-parallel geometry, provided interactions between the CO_2 subunits in a T-shaped configuration would differentially shift their vibrational frequencies by a resolvable amount.

A fully resolved $\nu_1 + \nu_3$ spectrum of CO_2 dimer was observed near 3714 cm^{-1} by Jucks et al.[118] with the bolometer technique, which permitted assignment of perpendicular ($\Delta K = \pm 1$) transitions from $K_a'' = 0$, 1, and 2 (see Table III). This observation immediately rules out a T-shaped structure for the dimer. For such a postulated geometry, K_a correlates with J of the "T" CO_2 subunit; nuclear spin statistics for the spinless oxygens in CO_2 would therefore preclude $K_a'' =$ odd in the dimer spectrum. IR Stark measurements yielded a null result for the dipole moment ($\mu < 0.04$ D), i.e., again inconsistent with a T-shaped geometry. Finally, asymmetric top fits to the assigned transitions in the spectrum were indeed consistent with a slipped-parallel geometry with vibrationally averaged values, $R_{CC} = 3.5$ Å and $\theta = 63°$, in excellent agreement with theoretical predictions.[163] However, the data could not be fit as a conventional asymmetric rotor to within experimental precision, suggesting that wide amplitude motion and/or tunneling may be occurring in the complex.

Experimental data on higher polymers of CO_2 would help elucidate some of these issues of relative stability of different conformations. Recently, Fraser et al.[120] have observed and analyzed the spectrum of CO_2 trimer near 3614 cm^{-1}, tentatively assigned to the $2\nu_2 + \nu_3$ component of the Fermi-coupled ν_1 and $2\nu_2$ states. Their analysis of the spectrum, particularly the absence of $K'' = 1, 2, 4, 5, \ldots$ levels resulting from spinless nuclei in a potential with 3-fold axis of symmetry convincingly indicates that the vibrationally averaged geometry is planar with C_{3h} symmetry. At first a cyclic structure might seem inconsistent with the slipped-parallel structure for the dimer; however, this minimum energy structure is semiquantitatively predicted by quadrupole–quadrupole plus hard-sphere interactions. Indeed, this model predicts stable cyclic conformations for higher polymers as well, but to date no high-resolution data on these structures have been observed and assigned.

5. $(N_2O)_n$

Spectroscopic observation of nitrous oxide polymers was first achieved in a jet-cooled molecular beam via the bolometer-based methods of Scoles and co-workers.[111] Laser excitation of the molecular beam near 2230 cm^{-1} results in a *depletion* of the bolometer signal on axis, indicating that the absorbing species predissociates on a time scale less than the time-of-flight travel between laser crossing and detector ($\sim 10^{-4}$ s). The spectrum was rotationally unresolved, but the identity of the absorber as nitrous oxide dimer was inferred from a quadratic power dependence of signal intensity on nozzle stagnation pressure. Later studies by Miller et al.[114] utilizing a mass spectrometer/bolometer combination demonstrated that under the previous experimental conditions the beams contained significant levels of high-polymer clusters up to $(N_2O)_{100}$ and suggested that the experimental line widths were dominated by rotational congestion and/or distribution in cluster sizes. This was shown to be the case by Miller and Watts,[166] who observed at much lower fractional N_2O/He seed ratios a dimer spectrum near 3500 cm^{-1} with discrete rotational structure, but at the time could not provide detailed assignments.

Huang and Miller[167] have exploited several enhancements of the bolometer sensitivity and F-center laser tuning to achieve the full rotationally resolved spectrum of N_2O dimer in the $\nu_1 + \nu_3$ combination band centered at 3478 cm^{-1} (see Table III). The spectra appear to be perturbed heterogeneously in the $K' = 0$ and 1 upper states, as evidenced by strongly asymmetric residuals in the fit. the J value of the crossing moves upward from $K' = 0$ to $K' = 1$; the lack of perturbed lines from the higher K states is presumably due to finite J population in the cooled molecular beam. Combination differences for the ground state provide the basis for evaluation of the vibrationally averaged structural parameters.

A 5:4 intensity alternation in transitions from the $K'' = 1$ submanifold arises from the nuclear spin statistics of the nitrogen atoms and provides definitive evidence for a center of symmetry in the intermolecular potential. This is completely consistent with the slipped-parallel dimer geometry observed in both CO_2[118] and HCCH.[162] It was not possible from the N_2O dimer data to distinguish between a slipped-parallel geometry with overlapping nitrogen or oxygen ends, but electrostatic model calculations predict both to be stable with a slight preference for the latter.

6. $(HCN)_n$

Complexes of hydrogen cyanide were first observed in low-resolution gas-phase infrared studies in static cells by Jones et al.[37] Fourier transform microwave experiments by Buxton et al.[98] were successful in inferring the linear, hydrogen-bonded structure of the ground-state dimer. Higher resolution laser-based experiments on HCN dimer and trimer were performed by Hopkins et al.[132] and Maroncelli et al.[133] utilizing photoacoustic Raman and infrared spectroscopy in static cells of HCN, as well as coherent anti-Stokes Raman spectroscopy (CARS) in a pulsed supersonic jet.

Although these spectra were not rotationally resolved, analysis of the band contours indicated a linear HCN dimer with rotational constants that decreased slightly upon vibrational excitation of the CN stretch. Most interestingly, the vibrationally averaged structure for the trimer was inferred from band contour analysis also to be linear. This result was in accord with the bulk-phase linear-chain structure observed for solid HCN,[168] as well as theoretical calculations that predicted a relative energy difference of 380 cm^{-1} between cyclic and linear forms.[169]

The first rotationally resolved vibrational data on HCN dimer were obtained by Wofford et al.[80] using long-path White cell, FTIR absorption methods. These authors report a hydrogen-bonded ν_2 (CH stretch) vibration at 3241.56 cm^{-1}, red shifted by 70 cm^{-1} from the HCN monomer and in good agreement with the findings of Maroncelli et al.[133] A predissociation/relaxation line width of 192 ± 40 MHz FWHM was estimated, though this required deconvolution of significant Doppler, pressure, and instrumental broadening contributions. This line width was reported to be independent of J and the magnitude consistent with estimates from a trapped collision pair model.[170]

Jucks and Miller[171] more recently have investigated the HCN dimer spectrum with sub-Doppler bolometric techniques and observe both the "free" and "bonded" CH stretch, ν_1 and ν_2, respectively, as well as some bending hot bands built on the ν_1 mode. the ν_1 vibration is red shifted by only 3.16 cm^{-1} from the monomer, and hence would have been unobservable in the lower resolution efforts of Maroncelli et al.[133] Jucks and Miller[171] report very small shifts in both the averaged geometry and dipole moment of the dimer upon ν_1 excitation, consistent with only weak interactions between the free CH and intermolecular degrees of freedom. This is corroborated by observation of instrumentally limited line widths ($\lesssim$1 MHz) in the ν_1 spectrum. In contrast, there is evidence for much stronger coupling of the ν_2 H-bonded CH stretch to the molecular framework. The ν_2 upper state appears to be severely perturbed, as indicated by large but identical residuals in the fit for P(J + 1) and R(J − 1) transitions. Sub-Doppler studies of the ν_2 vibration indicate measurable predissociation/relaxation line widths of 26-MHz FWHM, which is substantially narrower than the previous estimates of Wofford.[80]

Jucks and Miller[171] also observe three vibrational bands in the CH stretch region in HCN containing expansions, which they assign to the three CH stretches of the linear HCN trimer. The free H stretch frequency at 3306.80 cm^{-1} is very nearly at the HCN monomer origin and exhibits instrument-limited line widths ($\lesssim$1 MHz) corresponding to a minimum predissociation lifetime of 140 ns. The two H-bonded stretches, ν_2 and ν_3, are observed at 3231 and 3212 cm^{-1} and, based on calculations of Kofranck et al.,[169] are assigned as the asymmetric and symmetric combination stretch, respectively. Interestingly, the asymmetric stretch band exhibits completely unresolved structure whose band contour is best fit with a 0.5-cm^{-1} (=15 000 MHz!) FWHM, whereas the symmetric band is cleanly resolved, with predissociation/relaxation line widths of 56-MHz FWHM. If this excess line width in the ν_2 and ν_3 modes can be ascribed completely to predissociation, this would represent the most extreme example to date of nonstatistical, mode-specific photophysics.

Additionally, Jucks and Miller[171] observe yet another rotationally resolved band in HCN expansions whose analysis indicates an isomeric, cyclic trimer structure. Due to spectral overlap of the K manifold structure in a planar oblate top, the vibrationally averaged geometry of the cyclic trimer could not be well determined, but the fits are consistent with a benzene-like equilibrium structure with a 3-fold axis of symmetry. A final vibrational band is observed which is tentatively assigned to HCN tetramer, but the lack of resolvable rotational structure prevents definitive analysis.

7. $(NH_3)_n$

No high-resolution spectroscopic data on ammonia dimer were available until the very recent IR microwave studies of Fraser et al.[136] They utilized a CO_2 laser to pump transitions in the complex corresponding to the ν_2 umbrella mode vibration in the monomer and monitored depletion of the ion mass corresponding to $(NH_3)_2$ in a quadrupole mass spectrometer in double resonance with a saturating microwave field on a dimer transition. This method permits a determination of the homogeneous line width of the IR predissociation profile near 980 cm^{-1} and indicates that the previous measurements[25] of these line widths were contaminated by vibrational and/or rotational heterogeneity. Since predissociation was observed, the binding energy of NH_3 dimer must be less than the 980-cm^{-1} photon energy.

From an analysis of the associated microwave data for NH_3 dimer, several surprising conclusions can be drawn. First, Fraser et al.[136] inferred a vibrationally averaged structure in which the subunits are neither centrosymmetric nor do they exhibit a linear N–H ···N hydrogen bond; rather the two inequivalent subunits are tilted away from the center-of-mass axis by roughly 49 and 65°, respectively. These angles are inferred from projections of multipoles of the subunits onto the A inertial axis and are in good agreement with electronic structure calculations by Sagarik et al.[172] It is worth pointing out, however, that these experimental results are also at odds with electrostatic[173] and ab initio[174,175] calculations, though these efforts predict both extremes of a centrosymmetric and classical linear H-bonded structure. Liu et al.[173] argue that relatively flat, low-energy tunneling paths exist between equivalent, minimum energy geometries, and thus large-amplitude motion in the complex around a linear hydrogen-bonded geometry might lead to a vibrationally averaged structure consistent with experiment. The remarkable consistency of these structural angles with H/D substitution demonstrated by Nelson et al.,[137,138] however, indicates that vibrational averaging does not significantly shift the deduced geometry far from the equilibrium geometry.

In the studies of Nelson et al.[137,138] and Fraser et al.,[136] only molecules with a single internally rotating ammonia subunit are observed, for which no tunneling motion is discerned. This excitation appears to localize on one subunit and leads to a very simple rigid rotor like spectrum for the states observed. No evidence for either unexcited or symmetrically excited ammonia dimer subunits is obtained, and thus the data set rep-

TABLE IV. Summary of Vibrational Data for H_2–Rare Gas Complexes

species	ν_0/cm^{-1}	mode descrip	$(\nu - \nu_{monomer})/cm^{-1}$	B/cm^{-1}	$R_0/Å$	ref
H_2	4161.17	H_2 stretch				
Ne–H_2	4161.15	H_2 stretch	−0.02	0.577	3.99	51
Ar–H_2	4160.08	H_2 stretch	−1.09	0.566	3.94	50
Kr–H_2	4159.54	H_2 stretch	−1.63	0.515	4.07	50
Xe–H_2	4158.66	H_2 stretch	−2.51	0.470	4.25	50

resents only a small fraction of the states energetically accessible in the complex. It would be most interesting and helpful to have more of the states characterized, and to this end, high-resolution, tunable IR laser spectroscopy of the ammonia dimer could make fundamentally important contributions toward resolving these controversies.

B. Heterogeneous Complexes

1. H_2–M Complexes

(a) H_2–Inert Gas. Discussion of complexes of molecular hydrogen with inert gases deserves some special attention, since investigations of this class of molecules provided the very first rotationally resolved and assigned infrared spectroscopic data on weakly bound systems. Two key features made these pioneering studies experimentally tractable with only moderate resolution. (1) Molecular hydrogen is homonuclear and therefore has no dipole-allowed transition moment, whereas transitions in the complex can be allowed. This permits study at relatively high cell pressures of hydrogen, thereby facilitating complex formation without interference from monomer absorptions. (2) The reduced mass of the complexes is essentially that of H_2, yielding rotational constants on the order of 1 cm^{-1} and resolvable rotational structure with monochromator levels of resolution. The first observation of discrete spectral features in H_2 dimer in the near-IR was by Watanabe and Welsh.[47] Subsequent detection of rotational fine structure on the predominantly H_2 vibration (ν_1) in Ar–H_2 complexes near 4000 cm^{-1} was achieved by Kudian et al.[48] The key observation here was that the line widths of these discrete features were still pressure dependent, indicating narrow intrinsic line widths and hence extremely slow predissociation in the vibrationally excited state.

These studies prompted a more comprehensive investigation by McKellar and Welsh[50] of complexes of H_2 and D_2 with Ar, Kr, and Xe in a 165-m path length White cell cooled to 85–158 K (see Table IV). Since it was anticipated that the angular anisotropy of the intermolecular potentials would be small compared to rotational energy spacings in H_2, analysis of these first spectra was for nonrotating H_2 ($j = 0$) complexes in a purely isotropic potential. The origins of the spectra were red shifted 1–2 cm^{-1} with respect to free hydrogen, indicating a deepening of the isotropic well upon ν_1 excitation. The presence of anisotropy in the potential was evident, however, in the partially resolved splittings observed in transitions to or from $j > 0$ levels of hydrogen. Subsequent studies[51] of the corresponding complexes of Ne with H_2 and D_2 indicated a nearly free rotation of the diatom, and a sufficiently weak binding energy to permit rotational predissociation in the ground vibrational state.

An extremely detailed analysis of the spectral data was performed by LeRoy and Van Kranendonk,[176] who performed matrix quantum calculations for an adjustable form of the potential and iterated in order to best fit the spectrum. The full set of observed transitions in $\Delta v = 1$; $\Delta j = 0,\pm 2$; $j'' = 0,1$ could now be included in the fit for each inert-gas partner. The form of the trial potential was appropriate to a case of nearly free internal rotation, i.e., an expansion in Legendre polynomials with explicit dependence of the coefficients on both hydrogen and intermolecular bond length. These fits produce estimates of well depths ranging from 26 cm^{-1} for Ne to 67 cm^{-1} for Xe, but with $P_2(\cos\theta)$ anisotropic contributions roughly 15% of the isotropic component.

Much improved resolution (0.06 cm^{-1}) and absorption sensitivity subsequently permitted a reinvestigation these complexes at even lower pressures.[52] Most interesting were the observations of systematic line broadening from *rotational* predissociation in the upper state for the $j = 2 \leftarrow 0$ transitions in Ar–HD complexes. Additionally, anomalous line broadening was also observed in a single transition for Kr–H_2 complexes. From fits to the potential surface, LeRoy et al.[53] predicted that rotational predissociation contributions to the line widths would be appreciable for $j = 2 \leftarrow 0$ transitions in both HD–Ar and H_2–Kr. Hutson and LeRoy[56] extended these calculations[177,178] on the fitted surface of LeRoy and Carley[179] in an exact close-coupling formalism to predict transition by transition rotational predissociation line widths in very good agreement with the experimental data. Most importantly, examination of the predicted final state rotational distributions indicated that "product" hydrogen is formed predominantly in the highest energetically and symmetry allowed rotational states. A simple physical interpretation of this behavior is that energy remaining in rotation minimizes the amount necessary to deposit into relative translation of the fragments.[180] This nicely explains the more rapid predissociation in Ar–HD over Ar–H_2 or Ar–D_2 excited to $j = 2$, since the $\Delta j = -1$ channel is accessible in HD due to the lack of ortho/para symmetry.

The corresponding phenomenon of *vibrational* predissociation, whereby the energy in the H_2 vibration breaks the van der Waals bond, was similarly investigated via close-coupling calculations by Hutson et al.[55] As might be expected from the extreme frequency mismatch between the H_2 and van der Waals stretch vibration, this process is extremely inefficient, contributing to line widths at the much less than 10^{-6}-cm^{-1} level. A similar trend as in rotational predissociation was observed in the final states; i.e., there was a pronounced tendency to produce rotationally "hot" H_2, D_2, and HD in the highest energetically accessible levels accompanied by $\Delta j > 2$. Again, this reflects a propensity to limit the energy deposited into relative translation, even though a $P_2(\cos\theta)$ anisotropy term in the H_2/D_2 potential would only account for $\Delta j = 2$ in first order.

TABLE V. Summary of Vibrational Data for Complexes of HF with Diatomic, Triatomic, and Polyatomic Substituents

species	equilib geometry	ν_0/cm^{-1}	mode descrip	$(\nu - \nu_{monomer})$/ cm^{-1}	$\Delta\nu_{FWHM}$/ MHz	D_e/cm^{-1}	ref
HF		3961.4229					
H_2–HF	*a*	3950.1282	ν_2 HF stretch (ortho H_2HF)	−11.2947	6	300	185–187
D_2–HF	*a*	3949.5567	ν_2 HF stretch (ortho D_2HF)	−11.8662	<100[b]		189
		3948.0237	(para D_2HF)	−13.3992	<100[b]		189
H_2–DF	*a*	2896.5745	ν_2 DF stretch (ortho H_2DF)	−10.4	<100[b]		
OC–HF	linear	3844.0278	ν_1 HF stretch	−117.3951	190	1066	202, 211
N_2–HF	linear	3918.2434	ν_1 HF stretch	−43.1795	7.2	795	119, 128, 202
		3920.9599	$\nu_1 + \nu_5 - \nu_5$ (N_2 rock)	−40.4630	<50[b]		128
N_2–DF		2872.6446	ν_1 DF stretch	−34.3			189
OCO–HF	near linear	3909.3204	ν_1 HF stretch	−52.1025	136	1733	129, 206
		3906.3659	$\nu_1 + \nu_6 - \nu_6$ (CO_2 rock)	−55.0570			129
ONN–HF	linear	3900.0191	ν_1 HF stretch	−61.4038	110	550	130, 208
NNO–HF	bent	3878.1882	ν_1 HF stretch	−83.2347	720	2041	206, 209
C_2H_2–HF	T	3794.3646	ν_1 HF stretch	−167.0583	200		215
C_2H_4–HF	T	3781.735	ν_1 HF stretch	−179.688	480		217
C_3H_4–HF	nearly T-shape	3769.299	ν_1 HF stretch	−192.124	1400		217
C_2N_2–HF	linear	3808.1491	ν_1 HF stretch	−153.2738	1140		218

[a] Minimum in potential for T-shape, but extensive vibrational averaging occurs in the H_2 rotation. [b] Resolution apparatus limited by residual Doppler broadening in a slit jet.

Using a perturbation theory adaptation of the originally used[176] secular determinant method (SEPT), LeRoy and Hutson[181] reanalyzed the higher resolution data of McKellar et al.[50-52] With hyperfine resolved microwave data from Waaijer et al.[182] and differential scattering data from Buck et al.,[183,184] an improved fit of the potential energy surface was obtained for H_2/D_2 with Ar, Kr, and Xe. The potential was modeled again as a Legendre expansion, but with coefficients that have a short-range exponential and long-range $1/R^6$ and $1/R^8$ dependence on the internuclear spearation and a polynomial dependence on the H_2/D_2 bond extension. Although the fits indicate a predominantly isotropic interaction with 10–15% contributions from $P_2(\cos\theta)$ terms, the analysis revealed higher order anisotropy in the Kr–H_2 potential that was used to determined a small but statistically significant $P_4(\cos\theta)$ term in the expansion. These surfaces arguably represent the best presently available for any triatomic system as a function of all coordinates.

(b) H_2–HF. The high-resolution infrared study of complexes of hydrogen with inert gases by McKellar et al.,[50-52] coupled with the analyses of LeRoy et al.,[176,181] provides a highly detailed description of nearly free internal rotation in weakly anisotropic atom–diatom systems. In complexes of hydrogen with hydrogen fluoride, one might anticipate a significantly more anisotropic interaction, and hence a description intermediate between the free and rigid rotor limits.

There are no reported observations of the microwave spectrum of H_2–HF. There have been considerable electrostatic and ab initio calculations on H_2–HF and isotopomers by Bernholdt et al.,[185] who predict a T-shaped equilibrium geometry with the H in HF pointing into the H_2 bond. A 130-cm^{-1} barrier to H_2 rotation and 300-cm^{-1} van der Waals bond strength are calculated. From this potential surface, approximate rotational constants are calculated by expectation values over the intermolecular stretch wave function; however, torsional motion of the H_2 rotor is neglected.[185] It is worth noting that the rotational constant for H_2 ($B \sim 60$ cm^{-1}) is not small with respect to the size of the rotational barrier (130 cm^{-1}), and therefore such an approximation neglects considerable wide amplitude bending motion of the H_2.

High-resolution infrared spectra of H_2–HF complexes have been obtained recently by Lovejoy and Nesbitt[186] and Jucks and Miller,[187] the former via slit jet direct absorption of a tunable difference frequency laser, the latter via bolometric "optothermal" detection with a tunable F-center laser (see Table V). An extensive P, Q, and R branch spectrum is observed by Lovejoy and Nesbitt[186] near 3950 cm^{-1}, with each transition split into a doublet pattern reminiscent of a $K = 1 \leftarrow 1$ parallel band in an asymmetric top. Fits to a semirigid, Watson A-type Hamiltonian,[188] however, predict a molecular asymmetry that would require a physically unreasonable 1.2-Å increase in the H_2 bond length upon complexation. A more appropriate analysis, suggested by the small size of the calculated barrier to H_2 rotation, is in terms of a hindered internal rotor, which correlates in the separated limit with a free ortho $j = 1$ H_2. Sufficient concentration of rotationally excited ortho $j = 1$ H_2 monomers in the jet-cooled beam is ensured (indeed favored for a normal H_2 3:1 ortho:para distribution) by nuclear spin statistics, the distributions of which are not relaxed on the time scale of the expansion. From a quantum analysis of the splittings for fixed H_2–HF separation, one can extract barriers to internal rotation of 130–170 cm^{-1}, in good agreement with the calculations of Bernholdt et al.[185] These barriers are systematically very sensitive, however, to both vibrational and rotational state. A simple but accurate physical picture is one of a sterically hindered H_2 rotor, where the barrier to internal rotation decreases rapidly with intermolecular separation. This barrier therefore is strongly v and J quantum state dependent by virtue of (i) a shortening of the H_2–HF intermolecular separation upon HF excitation and (ii) centrifugal stretching of this separation with end-over-end rotation of the complex.

The sub-Doppler spectral resolution of the bolometer method permitted Jucks and Miller[187] to measure a predissociation line broadening of 6 MHz, which translates into a predissociation lifetime of 27 ns. Stark measurements on the lowest J transitions yield a dipole moment of 1.428 and 1.512 D in the ground and excited state, respectively. The approximately 0.2–0.3 D *decrease* in dipole moment from the free HF value suggests significant amplitude HF bending motion in the

TABLE VI. Summary of Vibrational Data for Complexes of HF and DF with Rare Gases

species	equilib geometry	ν_0/cm^{-1}	mode descrip	$(\nu - \nu_{monomer})/cm^{-1}$ exptl	theor	$\Delta\nu_{FWHM}$/MHz	D_0/cm^{-1}	ref
HF		3961.4229	HF stretch					
Ar–HF	linear	3951.7681	ν_1 HF stretch	−9.6548	−9.4	<0.0005[a]	102	64, 116, 125
		4009.100 (57.3319)[d]	$\nu_1 + 2\nu_2(\Sigma)$	+47.677				
		4022.1047 (70.3366)[d]	$\nu_1 + \nu_2(\Pi)$	+60.6818		<50[b]		64, 126
		4023.3380 (71.5699)[d]	$\nu_1 + 2\nu_3$	+61.9151				126
		3993.1030 (41.3349)[d]	$\nu_1 + \nu_3$	+31.6801				
		3954.4135	$\nu_1 + \nu_3 - \nu_3$	−7.0094		*c*		64
Ar–DF	linear	2897.9653	ν_1	−9.0		<40[b]		189
Kr–HF	linear	3943.9050	ν_1	−17.5179	−12.2	*c*	133	64, 196, 197
Xe–HF	linear	3932.2377	ν_1	−29.1852		*c*	181	64

[a] Inferred line width limited by time-of-flight path to bolometer. [b] Line width limited by residual Doppler broadening in a slit jet. [c] Line width limited by Doppler and pressure broadening in a cooled cell. [d] Frequency quoted in parentheses is for $(\nu_1 + \nu_{vdW}) - \nu_1$.

complex. The subsequent enhancement of dipole moment upon ν_1 excitation is consistent with a greater anisotropy in the upper state, corroborated by the increase in H_2 rotational barrier observed.[186]

The IR spectral data have been fit by iterative close-coupling calculations to a pseudotriatomic potential for the H_2 motion as a function of angular position and H_2–HF internuclear separation.[189] In contrast with the nearly isotropic H_2–inert gas potentials of LeRoy et al.,[176,181] the corresponding H_2–HF potentials are dominated by the $P_2(\cos\theta)$ anisotropic term, which is responsible for over $^2/_3$ of the binding energy in the complex. Interestingly, full close-coupling calculations for the para H_2–HF complexes indicate a much more weakly bound complex due to (i) torsional averaging of the $j = 0$ H_2 wave function over a predominantly anisotropic van der Waals well and (ii) the large zero-point contributions from the H_2–HF stretching vibration. This strongly quantum state dependent bonding may explain the lack of a detectable spectrum in either para H_2–HF or para H_2–DF,[189] as well as the easily observed spectrum of both ortho and para D_2–HF, for which more stable bound states are predicted due to a smaller zero-point energy in the stretch coordinate. However, consideration of coupled, large-amplitude motion in both the H_2 and HF bending degrees of freedom will be necessary to explain these behaviors quantitatively.

2. Hydrogen Halide–Inert Gas Complexes

Largely by virtue of their simplicity, hydrogen halide–inert gas complexes have served as a focus for much of the interaction between high-resolution experiment[43,64,65,125,126,135,139–141] and high-level theory,[190–195] and one in which the recent burst of IR experiments promises to make a profound contribution (see Tables II and VI).

When an atom and a diatom form a complex, one translational and three rotational degrees of freedom become, nominally, intermolecular stretch and bend vibrations, respectively. However, in such systems where wide-amplitude motion is important, these intermolecular vibrations are not far removed from the corresponding pure motion in the separated units! Consequently, some of the intuitions based on molecular spectroscopy of nearly rigid molecules require substantial reevaluation. For instance, the three bend vibrations are split by the anisotropy of the potential into a doubly degenerate out-of-plane bend ("perpendicular") and a nondegenerate in-plane bend ("parallel") with $l = 1$ and 0 projection of vibrational angular momentum along the inertial axis, respectively. The parallel bend strictly correlates with the HF bending overtone, which in a more rigid molecule would be nominally at twice the energy of the fundamental, perpendicular bend. However, in the hydrogen halide–inert gas complexes, where there is only a relatively weak anisotropy to the potential, these parallel and perpendicular bends are nearly degenerate. Indeed the spectroscopic data suggest that the parallel bend (overtone) in Ar–HF[189] and Ar–HCl[139,140] lies *beneath* the perpendicular bend (fundamental) due primarily to a secondary well in the inverted Ar–XH configuration which is not sampled by the perpendicular bend states, and hence justifying its colloquial name, "undertone".[43] Consequently, the relative ordering of these vibrational levels, as well as the couplings between these levels, provides important constraints for determining the shape of the intermolecular potential energy surface.

Second, the wide-amplitude motion in the bend and stretch coordinates modulates the normally allowed IR transitions in the subunits at the intermolecular mode frequencies and thereby leads to anomalously strong transitions in combination and difference bands. Indeed, the fundamental diatomic stretch transition in these complexes correlates with the Q branch in the free subunit and is therefore *only* allowed by virtue of anisotropy in the potential. The net result is that transitions built on the strong, near-IR mode in the hydrogen halide provide a rather direct probe of the much lower frequency, intermolecular modes. Alternatively one can investigate the low-frequency modes directly in the far-IR,[43,135,139–141] exploiting the fact that these vibrations carry oscillator strengths characteristic of rotational transitions in the free hydrogen halide.

(a) Ar–HF. The first spectroscopic evidence for Ar–HF complexes was observed in the near-infrared by Vodar and Vu[35] in the null gap region between R(0) and P(1) in HF monomer in high-pressure HF/Ar gas mixtures. A full decade later high-resolution microwave MBER experiments by Harris et al.[89] determined the ground-state vibrationally averaged geometry of Ar–HF and Ar–DF. These measurements were extended by Dixon et al.[92] Though the equilibrium geometry was

inferred to be linear, large zero-point motion in the wide-amplitude HF bending coordinate led to a vibrationally averaged angular displacement of 48° away from linearity. From the J-state dependence of these angular properties, as well as the centrifugal distortion of the centers of mass separation, approximate estimates of the low-frequency bend and stretch modes were made. These data were used by Hutson and Howard[193] to construct a potential energy surface, which predicted an Ar stretching vibration at 40 cm^{-1} and the parallel and perpendicular bend vibrations at 57 and 68 cm^{-1}, respectively.

The first high-resolution IR measurement on Ar–HF (see Table VI) was made by Lovejoy et al.[125,126] utilizing direct absorption of a difference frequency laser in a slit supersonic jet expansion. The ν_1 fundamental at 3952 cm^{-1} was red shifted by 10 cm^{-1} with respect to the monomer, indicating a tighter bonding in the upper state and in good quantitative agreement with calculations by Liu and Dykstra.[196,197] This is consistent with a decrease in center of mass separation of Ar and HF subunits inferred from a positive $\Delta B/B$ upon ν_1 excitation. The line widths in the sub-Doppler slit jet configuration were observed to be apparatus limited at <50 MHz FWHM.

In addition to the fundamental band, the $\nu_1 + \nu_2$ combination band was observed 70 cm^{-1} to the blue of the ν_1 origin,[126] in good agreement with the Hutson and Howard surface[193] predictions (ν_2 = 68 cm^{-1}) for the HF unexcited stretch state. A fortuitous crossing of the $\nu_1 + \nu_2$ manifold by rotational levels in another vibrational manifold resulted in an isolated $\Delta l = 1$ Coriolis perturbation in the P/R branches which could be assigned and completely analyzed. The perturbing state was determined to be $\nu_1 + 2\nu_3$, lying 72 cm^{-1} above the ν_1 origin and with a dramatically decreased rotational constant ($\Delta B/B = -20\%$) characteristic of high stretch excitation along the dissociation coordinate. The strength of this Coriolis interaction indicated significant coupling between bending and stretching states, as was also evidenced in the increase in van der Waals bond length upon excitation of the perpendicular bend.

Cooled White cell studies of Ar–HF complexes were performed by Fraser and Pine[64] using a tunable difference frequency laser. At these much warmer temperatures (211 K), both fundamental ν_1 and hot-band spectra in the low-frequency van der Waals stretching mode, $\nu_1 + \nu_3 - \nu_3$, were observed and analyzed. Stretching of the van der Waals bond clearly weakens the van der Waals interactions, and hence the hot-band origin, at 3954 cm^{-1}, is blue shifted by 2 cm^{-1} with respect to the fundamental back toward the free monomer transition. Interestingly, thermal rotational excitation is sufficient to predissociate the complexes; the spectra thus demonstrate abrupt cutoffs in the rotational progressions (J = 40 for ν_1, J = 31 for $\nu_1 + \nu_3 - \nu_3$). Fraser and Pine[64] use an angularly averaged analysis of the bound J states to fit radial potentials in the internuclear separation for each of the vibrations observed. This radial potential predicts the vibrational origin of the $\nu_1 + 2\nu_3$ state at 72.2 cm^{-1} above the ν_1 origin, with a rotational constant of 0.08264 cm^{-1}. This is in excellent agreement with the perturbing state analysis in the jet studies of Lovejoy et al.,[126] who determine the origin and rotational constant to be 71.6 and 0.0818 cm^{-1}, respectively. The well depths from this radial potential are 125 and 136 cm^{-1} in the HF ν_1 = 1 and 0 state, respectively. This deepening of the well is again consistent with the tightening of the van der Waals bond upon vibrational excitation.

Neither the slit jet[125,126] nor cooled White cell[64] spectra demonstrated any appreciable spectral line broadening that could be attributed to predissociation effects in excess of 50 MHz. These upper limits were dramatically reduced by the bolometer measurements of Huang et al.,[116] in which they found that the vibrationally excited complexes survived the full distance from the laser excitation region to the bolometer! Hence the signals corresponded to a *warming* of the beam rather than a predissociative *cooling* out of the collimated beam. From an analysis of the instrumental response, a lifetime lower limit of 3×10^{-4} s for the vibrationally excited state could be inferred. From a Stark analysis, an increase in dipole moment in the upper state was determined and attributed to reduced zero-point angular averaging of the HF dipole moment. A greater anisotropy, and hence more directed HF subunit in the upper state, is consistent with the previous discussion of enhanced intermolecular attractions upon ν_1 vibrational excitation.

Information on higher clusters of Ar and HF has been recently been determined by FT microwave studies by Gutowsky and co-workers. Rotationally resolved microwave spectra of Ar_2HF[198] and Ar_3HF (DF)[199] have been obtained. To date, however, there have been no published accounts of rotationally resolved infrared spectra of these or similar clusters.

(b) Kr–HF. The only high-resolution IR data on Kr–HF complexes (see Table VI) are from Fraser and Pine[64] using tunable difference frequency direct absorption in a cooled White cell. The origin of the ν_1 HF stretch was observed at 3943.9 cm^{-1}, 18 cm^{-1} red shifted from the monomer stretch, versus a 12.2-cm^{-1} red shift predicted by Liu and Dykstra.[196,197] The van der Waals stretch hot band is red shifted by only 14 cm^{-1}, similar to the behavior exhibited in Ar–HF. Rotational predissociation from levels above J = 54 was observed in the ground vibrational state. A one-dimensional radial analysis of the data yields a well depth of 157 cm^{-1}. No evidence for excess line broadening above the pressure and Doppler contributions was observed.

(c) Xe–HF. Again, the only high-resolution data on Xe–HF complexes (see Table VI) are those of Fraser and Pine,[64] who observed and assigned transitions from the fundamental ν_1 stretch at 3932 cm^{-1}, red shifted 29 cm^{-1} from the monomer. Due to a smaller rotational constant and deeper well resulting from the size and polarizability of xenon, thermal energy at 211 K was insufficient to populate states up to the rotational predissociation limit. Hot bands in the van der Waals stretch were observed but not assigned. Nonetheless, an estimate of 205-cm^{-1} well depth between Xe and HF was permitted by the wide range of J states detected.

(d) Ar–HCl. The story of research efforts on the Ar–HCl system is extensive, quite colorful, and still in a rapid state of evolution (see Table II). The first indications of an Ar–HCl complex were obtained by Turrell et al.,[200] who monitored absorption in the null gap between R(0) and P(1) in Ar/HCl mixtures. Partial spectral structure in this region was later observed by

Rank et al.,[33] the intensity of which increased upon cooling the cell. From a temperature dependence of this excess absorption, an enthalpy of formation for the Ar–HCl complex of 385 cm^{-1} was inferred.[34]

Theoretical scattering calculations on Ar–HCl were performed by Neilson and Gordon,[190] who as a prerequisite obtained an approximate potential in both the angular and radial coordinates by fits to transport data. This research stimulated experimental investigations on the Ar–HCl complex by Novick et al.,[88] utilizing the MBER technique. Analysis of the microwave rotational spectrum yielded an extremely nonrigid structure, with a linear equilibrium geometry but with a vibrationally averaged angular displacement of 42°. The dipole moments of the Ar–HCl complexes were found to *increase* upon deuteriation. This is consistent with a highly nonrigid angular potential in which zero-point motion averages out the projection of the HCl/DCl dipole along the internuclear axis. Analysis of the higher rotational levels, which by centrifugal distortion sample more extended intermolecular configurations, yielded a predicted van der Waals stretching frequency of 32.2 cm^{-1}.

The microwave data[88] were used to obtain a fit to the potential energy surface by Holmgren et al.,[151] who exploited the concept of a Born–Oppenheimer angular–radial separation (BOARS) of time scales to decouple radial and angular motion in a fashion analogous to Born–Oppenheimer separation of electronic and nuclear motion. Hutson et al.[152] extended this treatment to include perturbatively the angular–radial coupling terms in a corrected Born–Oppenheimer (CBO) formalism. The computational ease of these approximate but reasonably accurate treatments facilitated a fitting of the Ar–HCl potential surface by Hutson and Howard[191] to (i) MBER spectroscopic data, (ii) HCl pressure broadening data, (iii) virial coefficient studies, and (iv) molecular beam total differential cross sections. For an assumed form to $V(R,\theta)$, parameters in the potential could be adjusted to least-squares fit all the available data. Maitland–Smith potentials with coefficients that depended upon the angular coordinate proved the most satisfactory and predicted a minimum in the radial coordinate that decreased as the HCl is bent away from the linear geometry. A key feature of this so-called M3 surface is that the potential is quite flat near the inverted, Ar–ClH geometry.

Subsequent fits[192] to the corresponding Ne–DCl MBER data,[95] however, yielded a significant secondary minimum at the inverted Ne–ClD configuration. Additionally, ab initio calculations on the Ar–HCl surface suggested a similar minimum for the inverted complex. This prompted the fitting of an alternate semiempirical surface for Ar–HCl which exhibited a two wells with a barrier to internal rotational of 76 cm^{-1}. This M5 surface[192] was similar to the M3 surface in all other regions of the potential but more accurately reproduced the high-J infrared pressure-broadening data. The magnetiude of this secondary well, however, controls the relative energies of the parallel and perpendicular bending vibrations. The wave function for the parallel bend excited state extensively samples this back well, whereas the wave function for the perpendicular bend has a node in both collinear orientations. The microwave data on the ground state, however, could not provide that information; infrared data on the vibrationally excited levels were necessary to resolve this issue.

The first rotationally resolved infrared spectrum of an inert gas–hydrogen halide complex was obtained by Howard and Pine[65] for the ν_1 (HCl stretch) mode in Ar–HCl (see Table II). Tunable difference frequency laser direct absorption spectra in a 72-m, 127 K White cell yielded a rich fundamental ν_1 spectrum for both ^{35}Cl and ^{37}Cl isotopes with origins at 2884 and 2882 cm^{-1}, respectively. The 1.8-cm^{-1} red shift from the HCl monomer is in good agreement with low-resolution data of Rank et al.[33,34] and indicates an only small increase in binding energy upon HCl excitation. This is further supported by a small but definite *increase* in R_{cm} for Ar–HCl, in contrast with the definite *decrease* of R_{cm} observed in ArHF. An abrupt cutoff in the spectrum was observed at $J = 60$ and attributed to rotational predissociation in the ground state. A purely radial fit of the rotational eigenvalues and line widths to a Maitland–Smith potential was used to obtain a well depth estimate of 132 cm^{-1}, which differs substantially from the earlier estimates[34] based on temperature dependence of unresolved IR spectra for Ar–HCl. From this potential Howard and Pine[65] predicted the van der Waals stretching frequency at 31.3 ± 1.0 cm^{-1}.

The combination band of the ν_1 stretch with the perpendicular bend, $\nu_1 + \nu_2$, was observed by Howard and Pine[65] to the blue of the ν_1 fundamental transition at 2918.3 cm^{-1}, identifying the perpendicular bending vibration at 34 cm^{-1}. An extensive Q branch was observed which degraded to the blue and terminated abruptly near $J = 55$ ostensibly due to rotational predissociation. The corresponding R/P branch was stated to be strongly perturbed at low J, precluding an assignment of all but the R branch between $J'' = 22$ and 53. A strong unresolved feature at 2916.7 cm^{-1} could not be assigned, though it was determined definitely to result from Ar–HCl complexes. The analysis of the R-branch fragment in conjunction with the Q-branch data yielded a positive l-doubling constant of +34.2 MHz. Since the magnitude and sign of l-doubling are sensitive to the proximity and relative ordering of the Π perpendicular bend with Coriolis coupled Σ states, these data would suggest a nearby Σ state at higher energy.

Shortly thereafter, direct excitation of the ν_2 perpendicular bend was investigated by Marshall et al.[135] via far-infrared laser–Stark spectroscopy in a MBER apparatus. In this method, a line-tunable far-infrared (FIR) laser intersects a molecular beam of complexes which can be state selected by electrostatic focusing fields. Stark tuning of the complexes into resonance with the FIR laser alters the population of molecules in the observed state, which is detected mass spectrometrically. Spectra of several Stark resonances were observed which could be convincingly assigned to the perpendicular bending mode. The dipole moment of this state was measured to be 0.265 D, dramatically decreased from the 0.811-D value of the ground state due to large perpendicular tilting of the rotating HCl subunit. From an analysis of hyperfine structure, a vibrationally averaged angle of 60–80° was inferred. Interestingly, the l-doubling in this state was measured to be −49.6 MHz, in contrast with the +34.2 MHz value

of Howard and Pine[65] and suggesting that there might be a change in vibrational ordering of the low-frequency van der Waals modes between the HCl $\nu_1 = 0$ and 1 levels.

During the same period, Ray et al.[43] developed a method of investigating molecular complexes based on Stark-tuned, intracavity absorption of a line-tunable FIR laser in a supersonic jet. The high sensitivity of the Stark intracavity method permitted detection and assignment of many more rotational transitions; analysis of the Stark spectra yielded generally good agreement with the Marshall data, in particular, a comparable negative value for the l-doubling constant of −49.1 MHz. This magnitude was attributed to Coriolis interactions with the parallel bend vibration at lower energy. An origin for the perpendicular bend of 33.98 cm^{-1} was determined, which was essentially identical with the bending frequency inferred in the HCl excited state by Howard and Pine.[65]

Transitions to both the parallel and perpendicular bends in the HCl ground state were later observed by Robinson et al.,[139,140] utilizing microwave–far-infrared double-resonance techniques to assign the lower states unambiguously. The origin of the parallel bend at 23.66 cm^{-1} is significantly lower than the perpendicular bend at 33.98 cm^{-1} and reinforced the validity of the M5 potential surface. Indeed, the measured dipole moment for the parallel bend is −0.514 D, which is larger than and of opposite sign to that of the perpendicular bend, 0.265 D, due to a peaking of the wave function at the nearly inverted Ar–ClH configuration.

The van der Waals stretch mode, ν_3, was next to be observed by Robinson et al.[141] at 32.44 cm^{-1}, which is in excellent agreement with the predictions of Howard and Pine[65] from the HCl $\nu_1 = 1$ radial fit to the potential, as well as the early estimates of Novick et al.[88] from centrifugal distortion. Excitation of the van der Waals stretch dramatically decreases the vibrationally averaged rotational constants ($\Delta B/B = -10\%$), similar to the observations of the $2\nu_3$ mode in Ar–HF ($\Delta B/B = -20\%$).[126] The near resonance between the van der Waals stretch (32.44 cm^{-1}) and perpendicular bend (33.98 cm^{-1}) frequencies suggests that Coriolis coupling between these states is responsible for the large negative l-doubling observed in the perpendicular bend. This would be at least consistent with the considerable strength of absorption signal on the ν_3 mode, which would have a rather small transition moment in the absence of some coupling between the stretch and bend coordinates.

In a slit supersonic jet study using a tunable difference frequency laser, Lovejoy and Nesbitt[201] were subsequently able to observe all three van der Waals vibrations as combination bands built upon the ν_1 HCl stretch. The jet-cooled $\nu_1 + \nu_2$ spectrum exhibits a Q branch that agrees quantiatively with the reported frequencies of Howard and Pine.[65] However, the P and R branch observed in the supersonic jet is completely uncongested and yet qualitatively different from the previous measurements. Each transition can be assigned to the $\nu_1 + \nu_2$ band from ground-state combination differences. Analysis of the spectrum yields a negative l-doubling constant of −53.7 MHz and a vibrational origin 34.0548 cm^{-1} above the ν_1 level, virtually identical with the values obtained for the ground state. Interestingly, the jet-cooled spectrum exhibits a collapse of adjacent line spacing in the P branch near 2916.7 cm^{-1}, which suggests that the strong unassigned feature in the White cell spectrum is an unresolved P-branch head at the much higher (127 K) rotational temperatures.

The best fits to the $\nu_1 + \nu_2$ spectrum, however, require nonphysically high-order terms in a $J(J + 1)$ expansion and suggest that the rotational term values are being pushed upward by a perturbing state at lower energy.[201] Analysis of these levels reveals that there is significant Coriolis coupling between the perpendicular band and the van der Waals stretch. This strong coupling is partially responsible for generating oscillator strength in the $\nu_1 + \nu_3$ band, whose origin is determined to be at 32.64 cm^{-1} above ν_1.[201] By virtue of the significantly smaller B constant for the stretch than the bend mode and the fact that the stretch origin is beneath the perpendicular bend, the two rotational manifolds never cross and thus an isolated perturbation is not exhibited. Nonetheless, the coupling matrix elements grow with $[J(J + 1)]^{1/2}$, and hence the levels repel progressively more as a function of J, accounting for the anomalous P-branch band head behavior in the $\nu_1 + \nu_2$ spectrum. It is worth noting that such Coriolis interactions are most likely present in the ground-state studies as well. It would be interesting to compare the magnitude of the Coriolis coupling of stretch and bend states from a similar analysis of the ground-state vibrational interactions.

Finally, the parallel bend mode is observed directly as a combination on the ν_1 spectrum, with an origin 23.63 cm^{-1} above the ν_1 fundamental. A summary of the upper and lower state spectroscopic properties of the low-frequency van der Waals vibrations is shown in Table II. The agreement between the two sets of data is remarkable, suggesting that excitation of the HCl stretch has a rather small effect on the intermolecular potential energy surface.

3. HF–Diatomic and HF–Triatomic Complexes

(a) N_2–HF. The first rotationally resolved observation of N_2–HF complexes was by Flygare and co-workers[99] in a Fourier transform microwave apparatus which indicated a linear equilibrium geometry. Electrostatic calculations by Benzel and Dykstra[202] on N_2–HF predicted a well depth of nearly 800 cm^{-1} and a van der Waals stretch frequency in good agreement with a pseudodiatomic analysis of the microwave data.[99] The low-freuency bending vibration was calculated to be similar to that of OC–HF, for which experiments also suggested a linear geometry.[100]

Partial rotational resolution in an OPO infrared laser vibrational predissociation spectrum of N_2–HF was obtained by Kolenbrander and Lisy,[23] who determined a ν_1 band origin at 3918 cm^{-1}, 43 cm^{-1} red shifted from the monomer value (see Table V). Much higher resolution experiments on the ν_1 band of N_2–HF by Jucks et al.[119] indicated line broadening on N_2–HF transitions of only 7.2-MHz FWHM. Stark measurements on the low-J transitions yielded a dipole moment of 1.991 and 2.106 D in the lower and upper state, respectively. Slit supersonic expansion absorption experiments by Lovejoy and Nesbitt[128] on N_2–HF in a slit jet permitted detection of transitions from $J \leq 37$. Pseudodiatomic

analysis of the rotational and centrifugal distortion data indicated a deeper well and shorter equilibrium separation upon vibrational excitation, consistent with similar observation in many other HF complexes. In these relatively warmer slit jets ($T_{rot} \sim 26$ K), hot-band spectra from thermally populated low-frequency ν_6 bending states were also observed. The 2.7-cm^{-1} blue shift of the bending hot band from the fundamental is consistent with a weakening of the hydrogen bond upon bend excitation, and hence a shift back toward the free monomer stretch value. Both intensity measurements and analysis of the *l*-doubling permit an estimate of the bend frequency at 85 ± 20 cm^{-1}. Quite recently, Lindeman et al.[203] extended these IR measurements to the four nitrogen isotopomers of N_2–HF, in an effort to determine whether a one-dimensional, isotopically invariant potential can reproduce each of the ν_1 rovibrational spectra.

(b) OCO–HF. The story of OCO–HF complexes provides an interesting example of how IR and microwave techniques provide important complementary information on the intermolecular potentials. Klemperer and co-workers[97] were the first to observe rotational spectra of OCO–HF complexes using an MBER apparatus. A linear, hydrogen-bonded equilibrium geometry was inferred from their analysis. Studies on OCO–HCl also yielded a linear equilibrium geometry for the complex. These were surprising results, since the sp^2 hybridization of the oxygen atom generates off-axis electron density for bonding with a Lewis acid such as HF or HCl. Indeed, parallel studies of the N_2O–HF complex by Klemperer and co-workers[96] indicated a decidedly bent structure, with hydrogen bonding to the oxygen terminus.

Direct IR observation in slit supersonic jets of the ν_1 HF stretch in OCO–HF complexes at 3909 cm^{-1} was obtained by Lovejoy et al.[129] The 57-cm^{-1} red shift from the monomer value could be predicted from electrostatic analysis for an anharmonic HF oscillator, in the spirit of Liu et al.[196,197,204] Based on a Voigt analysis of the absorption profiles, homogeneous line broadening in OCO–HF was measured to be 136 MHz FWHM, i.e., nearly 20-fold larger than in N_2–HF.[119]

Although the rotationally resolved transitions are in excellent agreement with the microwave studies of the ground state, there are several puzzling features of the OCO–HF IR spectrum. First, the ground-state centrifugal distortion value is 4–5 times larger than that of N_2–HF, for which a comparable binding energy might be anticipated; normally, one would associate larger centrifugal distortion effects with a softer stretching potential. Second, both the rotational and centrifugal distortion constants *increase* on ν_1 vibrational excitation. A positive $\Delta B/B$ is associated with a *strengthening* and shrinking of the hydrogen bond; a positive $\Delta D/D$ in a linear complex, however, suggests a *weakening* of the hydrogen bond. Lovejoy et al.[129] argue that these observations are consistent for a nearly linear OCO–HF complex with a very flat bending potential for the low-frequency intermolecular CO_2 rocking mode. This is in good agreement with calculations on OCO–HF by Hurst et al.,[205] which predict a bend potential that is flat to within 50 cm^{-1} over the first ±20°.

In support of this interpretation, hot-band spectra in the low-frequency bend mode are observed, from which one can estimate a bending frequency of 10 ± 5 cm^{-1}, i.e., nearly an order of magnitude smaller than for N_2–HF. The analysis of Lovejoy et al.[129] predicts large-amplitude zero-point motion (20–30°) in the CO_2 rocking coordinate, which is surprisingly large for motion of relatively heavy atoms. It would be interesting to obtain hyperfine information on these bend excited states from MBER spectra of the *l*-doublets and thereby elucidate more of the vibrationally averaged behavior in these wide-amplitude modes.

(c) N_2O–HF. A test of these simple ideas of sp versus sp^2 bonding with HF can be found in the study of HF complexes with N_2O, in which two distinct isomers are observed.[96,130] As stated above this complex was first studied by Klemperer and co-workers[96] in an MBER apparatus and determined to have a bent equilibrium structure with the HF hydrogen bonding on the oxygen atom. Theoretical calculations[206] on this system confirmed a minimum energy configuration at the bent geometry. High-resolution IR spectroscopy by Lovejoy et al. on the ν_1 HF stretch mode in N_2O–HF,[130] however, yielded a spectrum of a *linear* ıydrogen fluoride–nitrous oxide complex, red shifted by 61.4 cm^{-1} from the monomer and with fundamentally different ground-state rotational constants than observed previously in the microwave (see Table V). Subsequent investigation of complexes labeled with [^{15}N]nitrous oxide unambiguously demonstrated that the hydrogen bond in these complexes was forming on the nitrogen atom. This behavior in N_2O–HF complexes constituted the first demonstration of two stable geometric isomers in a hydrogen-bonded system. Subsequently, the linear isomer has been observed and verified experimentally in a FT microwave spectrometer,[207] as well as theoretically supported by electrostatic calculations.[208] The heavily blended IR spectrum of the bent isomer has also been recently observed by Miller and co-workers,[209] with a band origin red shifted by 83.2347 cm^{-1} and with homogeneous line broadening of 720 MHz FWHM.

(d) OC–HF. There have been extensive microwave studies on OC–HF and isotopically substituted complexes by Legon et al.,[100] and later by Campbell et al.[102] and Read and Campbell.[103] The equilibrium geometry has been inferred to be linear, with the HF hydrogen bonding to the carbon end of CO. A moderate-resolution infrared spectrum of the ν_1 HF stretch of OC–HF at 3844 cm^{-1} was obtained by Kyrö et al.[67] using a mode hop scanned F-center laser in a long-path absorption cell. This value of the vibrational origin is in fair agreement with recent calculations of Botschwina.[210] The homogeneous contribution to the line widths was estimated at 900–1500 MHz; however, these relatively warm spectra were significantly congested by rotational and low-frequency hot-band structure.

A much higher resolution spectrum of OC–HF was obtained by Jucks and Miller[211] in a cooled jet, in which the homogeneous line widths were determined to be 190 MHz FWHM. A careful study indicated a negligible *J*-state dependence to the observed line widths, except in the vicinity of $J' = 7$. Here they observe a splitting of rotational lines in the P and R branch that terminate near $J' = 7$ and analyze these splittings in terms of a vibrational perturbation in the excited state. Interestingly, the widths of these perturbed lines are proportional to their integrated intensity, which is nicely

shown to be consistent with an analysis of a predissociating and metastable vibrational state which cross rotational manifolds near $J' = 7$. From other perturbations evident in the spectra, at least three near-resonant vibrational states are inferred. If the CO stretch in the complex is close to the monomer value (2143 cm^{-1}), then the perturbing states must contain 3844 – 2143 cm^{-1} = 1701 cm^{-1} of energy in the low-frequency van der Waals modes, which would imply strong coupling between ν_1 and combination states with *multiple* vibrational quanta. In systems with small-amplitude motion, strong couplings between states differing by more than two quanta would not be anticipated.[212] However, Coriolis interactions with three-quanta changes are observed between stretch and bend states in Ar–HF[126] and it is therefore conceivable that the large-amplitude vibrational motion may account for such extreme behavior in OC–HF. It is also possible that the CO stretch overtone in the complex might be red shifted from the monomer value closer into resonance with ν_1 and thereby require only small-quanta excitation in van der Waals modes to account for the coupling. It would be interesting to measure this CO stretch frequency directly. Ab initio calculations by Botschwina,[210] however, predict even a blue shift (+43 cm^{-1}) of the CO stretch upon complexation.

4. HF–Hydrocarbon Complexes

(a) C_2H_2–HF. Microwave spectra of C_2H_2–HF complexes have been obtained by both MBER[213] and Fourier transform[214] techniques; these studies indicate a T-shaped vibrationally averaged geometry with the HF hydrogen bonded onto the CC triple bond. A partially rotationally resolved IR spectrum of the ν_1 HF stretch mode in this complex was observed at 3793.4 cm^{-1} by Kolenbrander and Lisy[23] utilizing laser-induced vibrational predissociation with an optical parametric oscillator (OPO)[3] (see Table V). The ν_3 CH stretching frequency was also observed at 3265 cm^{-1}. The resolution of the data did not permit any differentiation between excited- and ground-state molecular constants.

Full sub-Doppler resolution spectra of the ν_1 stretch were obtained by Huang and Miller[215] using the bolometer method. Analysis of the asymmetric top spectra yields a vibrational origin at 3794.3646 cm^{-1}, in fair agreement with the earlier results.[23] Nuclear spin statistics on the acetylenic hydrogens produce an alternation in the J intensities that permitted unambiguous assignment of a C_2 axis of symmetry in the potential surface. The observed A constant of the complex is very close to the B rotational constant of the monomeric acetylene, supporting a T-shaped vibrationally averaged geometry. Line widths in the HF stretch mode were determined to be 200 MHz FWHM. Stark studies determined a dipole moment in the upper state of 2.559 D, which is significantly larger than the ground-state value of 2.368 D. This could arise from a decrease in the wide-amplitude HF bending motion in the complex from 20 to 10°, but this effect would be much larger than observed in inert gas–HF complexes, and suggesting that enhanced charge exchange in the upper vibrational state may be important as well.

(b) C_2H_4–HF. C_2H_4–HF complexes were first studied by microwave methods,[216] from which their averaged structure was known to be T-shaped, with the HF hydrogen bonded to the CC double bond. Later studies by Kolenbrander and Lisy[23] in the infrared determined a ν_1 HF stretch frequency of 3781 cm^{-1}, as well as ν_9 and ν_{11} CH stretch frequencies at 3102 and 2986 cm^{-1}, respectively. A much higher resolution IR spectrum of the ν_1 HF stretch mode was obtained by Huang and Miller,[217] who observed nearly fully resolved K structure in the P, Q, and R branches. Fits to the spectra indicate an intensity alternation due to spin statistics characteristic of a C_2 axis of symmetry in the potential and consistent with a T-shaped geometry in both upper and lower states. Line broadening in C_2H_4–HF is observed to be 480 MHz FWHM, significantly larger than in C_2H_2–HF complexes. Stark measurements of the dipole moment again indicate a significant increase upon vibrational excitation (from 2.38 to 2.61 D), which is attributed to both a decrease in HF bending amplitude and a possible enhancement of charge exchange upon vibrational excitation.

(c) C_3H_4–HF. The only experimental observation at high resolution of the C_3H_4–HF complex is by Huang and Miller.[217] As is clearly the trend, the line widths in this complex are significantly broader than in acetylene–HF or ethylene–HF complexes and were estimated to be 1400 MHz FWHM. The spectrum, obtained by mode hop scanning an F-center laser, exhibits P, Q, and R branch structure, but with heavily blended K rotational substructure which precludes a quantitative fit. However, simulation of the spectra is consistent with a nearly T-shaped, hydrogen-bonded structure, but with some lateral displacement of the HF away from the central carbon atom.

(d) C_2N_2–HF. The rotational spectrum of this complex was obtained by Legon et al.[101] using FT microwave techniques; the analysis of the data was consistent with a vibrationally averaged linear structure. The high-resolution infrared spectrum of the ν_1 HF stretch at 3808 cm^{-1} was obtained by Jucks and Miller[218] via bolometric methods. Considerable homogeneous broadening was evident in the spectra; a predissociation/relaxation line width of 1140 MHz FWHM was measured. Linear fits of the spectra yielded large systematic residuals symmetric around the upper state value of J. In addition, irregularities in the intensities and line widths were observed, suggesting rotational state-dependent perturbations present in the upper state arising from either Coriolis or anharmonic couplings between vibrational levels. A lack of knowledge of the other vibrational modes as well as the broad spectral lines precluded a definitive analysis and assignment of the perturbing states.

5. HCN–Hydrogen Halide Complexes

(a) HCN–HF. HCN–HF has been an extensively studied complex and is the first polyatomic system for which data on each vibrational mode have been obtained (see Table VII). In what the reader can now see as a fairly well-established pattern, the first observation of HCN–HF complexes was in a low-resolution IR spectrum of this complex in a long path length cell by Thomas.[219] When two linear molecules form a linear (bent) complex, three translational degrees and two (three) rotational degrees of freedom correlate with intermolecular vibrations, respectively. From the low-resolution IR spectrum, Thomas[219] was able to identify

TABLE VII. Summary of Vibrational Data for HCN–HF Complexes

species	ν_0/ cm^{-1}	mode descrip	$(\nu - \nu_{monomer})$/cm^{-1} exptl	theor	$\Delta\nu_{FWHM}$/ MHz	ref
HF	3961.4229	HF stretch				
HCN	3311.473	CH stretch				
	2096.855	CN stretch				
	713.461	HCN stretch				
HCN–HF	3716.2116	ν_1 HF stretch	−245.22	−127	2722	68, 78, 209, 220
	3310.3284	ν_2 CH stretch	−1.144	−13	11.8	209, 220
	2120.935	ν_3 CN stretch	+24.080	+12	558	73, 220
	168.33	ν_4 vdW stretch				78
	726.5312	ν_5^1 HCN bend	+13.070			76
	550.0285	ν_6^1 HF rock				75
	76.1713	ν_7^1 HCN rock				78
DF	2906.9	DF stretch				
DCN–DF	2730.8909	ν_1 DF stretch	−176.1			77
	2638.1309	ν_2 CD stretch	+8			77
	1943.0046	ν_3 CN stretch	+18			77

three intermolecular modes, the two doubly degenerate bending modes which correlate in the separated limit with free rotation of each of the subunits (ν_6 and ν_7) and the nondegenerate stretching mode (ν_4), from which one could infer a linear equilibrium geometry for the complex. Later high-resolution measurements in the microwave domain by Legon et al.[13,14] in an equilibrium cell provided precision values for the ground-state vibrationally averaged structure, as well as for many low-lying vibrationally excited states appearing as "satellites" on the ground-state rotational transitions. From relative intensity measurements of these satellite transitions, in addition to analysis of the Coriolis effects exhibited in the l-doubling studies of the degenerate bend modes, estimates of the intermolecular vibrations were found to be in fair agreement with the low-resolution IR work.

High-resolution IR studies of HCN–HF have subsequently been pursued by Bevan and co-workers using a variety of experimental techniques that have mapped out the full vibrational manifold of the complex in considerable detail. In the first of these studies, Wang et al.[66] utilized a multimode F-center laser at 0.2-cm^{-1} resolution to monitor the ν_1 (nominally, HF stretch) band at 3714 cm^{-1} in a room temperature cell. Though rotational resolution was not achieved in these first attempts, P-branch band heads on each of a long series of sequence bands were observed and assigned to hot bands in the ν_7 intermolecular bend. With the incorporation of an etalon in the F-center cavity and mode hop scanning the laser, Kyrö et al.[68] reinvestigated the ν_1 band and were able to achieve rotational resolution on the fundamental ν_1 and first hot band, $\nu_1 + \nu_7 - \nu_7$. Notable was the significant increase in rotational constant upon ν_1 excitation, which was attributed to a shrinking of the hydrogen bond by 0.034 Å in the excited state, as well as the broad line widths observed (1800–2700 MHz) that were independent of cell pressure and greatly in excess of the Doppler and/or laser line width contributions. A more recent sub-Doppler measurement by Dayton et al.[209] indicates homogeneous line widths of 2722 MHz FWHM.

The ν_3 (CN stretch) mode of HCN–HF was observed at 2121 cm^{-1} soon thereafter by Wofford et al.[73] using FTIR techniques with 0.004-cm^{-1} resolution. Interestingly, whereas the HF stretch *red* shifts by −245.22 cm^{-1}, the CN stretch *blue* shifts by +24 cm^{-1} upon complexation. This is in good agreement with the work of Curtiss and Pople,[220] who had previously performed ab initio calculations at the SCF level and predicted an elongation and shortening of the HF and CN bonds, respectively, in the complex. The homogeneous line widths were measured to be much lower than for ν_1 excitation (500 MHz), after correction for Doppler and pressure broadening, which suggested a mode-dependent predissociation or intramolecular relaxation rate.

The intramolecular HCN bending mode, ν_5, was investigated by Wofford et al.[76] in a FTIR and White cell combination. The observed origin at 726.5 cm^{-1} was blue shifted from the 713.5-cm^{-1} value for the HCN monomer, also in fair agreement with the Curtiss and Pople[220] predictions. For a $\Pi \leftarrow \Sigma$ band, P/R branch transitions access one set of the doubled upper state levels (e levels), while the Q branch transitions access the complementary set (f levels). A lack of assignable rotational structure on the badly resolved Q branch, therefore, prevented any analysis of the l-doubling in this bending mode.

The last of the intramolecular modes, ν_2 (nominally the CH stretch), was observed by Kyrö et al.[69] using a continuously tunable, single-frequency F-center laser. The origin at 3310 cm^{-1} is little shifted from the monomer value of 3314 cm^{-1}, as predicted by Curtiss and Pople.[220] Hot bands in the ν_4 (intermolecular stretch) and ν_7 (HCN intermolecular bend) were also observed and analyzed. Excess line width of the transitions was determined to be 25 ± 8 MHz, though this required removal of a large 161-MHz Doppler contribution by computer deconvolution. Later sub-Doppler measurements by Dayton et al.[209] indicate the line widths to be 11.8 MHz FWHM for the ν_2 mode. This is significantly smaller than observed for either ν_1 or ν_3 modes, in support of the previous assertion of mode-specific relaxation and/or predissociation in the complex.

The ν_6 mode (HF intermolecular bend) was observed by Wofford et al.[75] at 550 cm^{-1} in an FTIR apparatus with 0.01-cm^{-1} resolution. This is in good agreement with the initial low-resolution data by Thomas.[219] Rotational analysis indicates that the hydrogen bond length grows upon excitation of the bend, which is consistent with a weakening of the hydrogen bond as the HF is tilted off axis. A similar phenomenon is observed in Ar–HF complexes[125,126] and indicates a significant degree of coupling between the stretch and bend vibrational manifolds.

Explicit indication of these bend–stretch couplings is evident in a reinvestigation of the ν_1 spectrum by Bender et al.,[78] who discovered and successfully ana-

lyzed several isolated perturbations in the rotational term values, some of which could be assigned to Coriolis interactions with ν_7 bending and ν_4 stretching combination vibrations. In addition, the difference band $\nu_1 - \nu_4$ was observed, which permitted the ν_4 stretching frequency at 168 cm^{-1} to be inferred.

Finally, overtone spectra of HCN–HF have been observed in two of the modes, ν_1 (HF stretch) and ν_5 (HCN intramolecular bend),[74] as well as several hot bands built upon them. These data provide information on the anharmonicities of the modes, and in conjunction with the considerable data on the other vibrations in the complex, permit an approximate harmonic stretching force field to be determined.[74]

Parallel investigations in DCN–DF were performed by Jackson et al.[77] A similar trend in frequency shifts upon complexation (i.e., $\Delta\nu_1 = -176$ cm^{-1}, $\Delta\nu_2 = +8$ cm^{-1}, $\Delta\nu_3 = +18$ cm^{-1}) is observed. Of particular interest is the isotopic dependence of the predissociation/relaxation line widths for each of the modes investigated. For ν_1 and ν_3, the line widths *decrease* upon deuteriation. This is consistent with the similar behavior observed in HF and DF dimer and is qualitatively inconsistent with earlier, collinear dissociation models that predict an increase in the predissociation rate for a nearer resonance between the excited and dissociating mode.[16] The line widths for the ν_2 mode, however, *increase* upon deuteriation. One must remember that the ν_2 mode was the least efficient of the three at promoting predissociation/relaxation in the complex. Therefore, this apparently anomalous behavior may be attributed simply to the much stronger, more nearly resonant mixing of the CN and CD stretches in DCN over the corresponding modes in HCN. Interestingly, the trapped collision pair model proposed by Lieb and Bevan[170] to explain line widths in HCN–HF, OC–HF, and HCN dimer, which relies on an intermolecular V–V transfer process, fails by 4 orders of magnitude for the DCN–DF complex.

(b) HCN–HCl. Pulsed Fourier transform methods by Legon et al.[104] were first used to obtain the microwave rotational spectra of HCN–HCl complexes. Bender et al.[79] obtained an infrared absorption spectrum of HCN–$H^{35}Cl$ by tunable F-center laser absorption spectroscopy in a 144-m path length White cell. The $\nu_1 = 1 \leftarrow 0$ transition near 3309 cm^{-1} was observed and assigned; in addition, a series of hot bands in the same region were tentatively assigned to a sequence in the $\nu_1 + n\nu_7 - n\nu_7$ HCN rocking mode. Analysis of the l-doubling in the sequence band suggests a ν_7 frequency of 41 cm^{-1}; a pseudodiatomic analysis of centrifugal distortion indicates a ν_4 stretch frequency of roughly 100 cm^{-1}.

6. Polyatomic–Inert Gas Complexes

(a) OCS–Inert Gases. The first rotationally resolved data on carbonyl sulfide complexes with inert gases were obtained from MBER studies on OCS–Ar by Harris et al.[90] and indicated a nearly T-shaped vibrationally averaged geometry, with the Ar slightly shifted toward the oxygen. A stretching frequency of 36 cm^{-1} was roughly estimated from centrifugal effects. More recently, the series OCS–Ne, OCS–Ar, OCS–Kr has been investigated by using Doppler-limited, direct absorption infrared spectroscopy in a cooled molecular beam with a tunable diode laser[121,122] (see Table III). Indeed, this study marked the first direct absorption measurement of complexes in a supersonic jet and was the precursor to several methods described in this review. Predominantly B-type transitions were observed, which is consistent with a transition moment along the OCS and perpendicular to the A axis. A rigid rotor Hamiltonian fit to these transitions yields rotational constants that are consistent with a nearly T-shaped average structure for both ground and excited states. The data do not distinguish to which side the Ar is shifted, but a shift toward the oxygen end predicts nontouching van der Waals radii and is consistent with the ground-state microwave information on OCS–Ar.[90] Neither microwave nor IR investigations provide any quantitative information on the frequency of the bending potential, which would be particularly useful to assess the degree of wide-amplitude motion involvedd in these vibrational averages.

The shift of the vibrational origins from the monomer value is <1 cm^{-1} and varies systematically in sign between the blue shift in OCS–Ne (+0.12 cm^{-1}) and the red shifts in OCS–Ar and OCS–Kr (–0.46 and –0.86 cm^{-1}, respectively). These spectral shifts correlate strongly with polarizability of the inert gas, but the correct model for this interaction is not clear. In any event, the small magnitude of these shifts suggests weak coupling of the ν_3 excited mode and the binding energy of the complex. This is consistent with a long vibrationally excited lifetime (in excess of 10^{-9} s), and the observation of fully Doppler-limited line widths in the expansion. This result seems somewhat surprising in light of the extremely short lifetimes (5×10^{-12} s) deduced from CO_2 laser vibrational predissociation studies of $2\nu_2$ excited OCS–Ar by Hoffbauer et al.,[221] though this bending mode in a T-shaped complex may have substantially more displacement along the dissociation coordinate. If experimentally feasible, it would be interesting to see the results of a direct absorption tunable IR laser experiment on this $2\nu_2$ mode in OCS–Ar with which to make a more direct comparison of the dynamical behavior.

Hayman et al.[122] have utilized microwave–IR double-resonance techniques to explore the rotational spectroscopy of the ground vibrational state of these inert gas–OCS complexes at much higher resolution than conventionally accessible from infrared laser methods. The authors warn that their analysis of the data is based on a rigid rotor model and that the small differences in effective structures observed between members of the series may well be accounted for by large-amplitude vibrational averaging in the bend and/or stretch coordinates. In principle, this technique could be extended to study the high-resolution rotational spectroscopy of the vibrationally excited states, much as Muenter and co-workers[222] have performed for several stable molecules. Provided sufficient IR power is available to change appreciably the quantum state populations, this method could also be used as a sub-Doppler probe of the predissociation lifetimes of the upper state. In an interesting reversal of the normal trend, these IR-based studies facilitated the spectroscopic search for OCS–Kr and OCS–Ne complexes in FT microwave experiments by Lovas and Suenram,[223] which now have determined the ground-state molecular

properties in this series to high precision.

(b) N_2O–Ar. High-resolution spectra on N_2O–Ar complexes were first obtained in the microwave by Joyner et al.[224] utilizing MBER techniques. An approximately T-shaped vibrationally averaged geometry was inferred from the rotational and hyperfine constants. Hodge et al.[123] have subsequently obtained rotationally resolved infrared spectra of the nitrous oxide–argon complexes via direct absorption of a diode laser in a pulsed supersonic jet. The origin of the band at 2223 cm^{-1} is blue shifted by +0.15 cm^{-1} with respect to the free monomer ν_3 transition, which suggests a slight decrease in binding energy and hence an increase in repulsive interactions in the vibrationally excited state. The rotational constants show very small changes upon vibrational excitation. Only B-type ($\Delta K_a = \pm 1$, $\Delta K_c = \pm 1$) transitions were observed; this is consistent with a T-shaped averaged geometry, since the ν_3 transition moment in N_2O would then be perpendicular to the *A* inertial axis. Given the very slight coupling experimentally observed between ν_3 excitation and average molecular structure, a vibrationally metastable complex might be expected. Indeed, the line widths were measured to be limited by a combination of Doppler broadening and laser frequency jitter contributions to below 100 MHz FWHM. It would be very interesting to obtain information on the low-frequency rocking modes of the complex to comment further on the extent of vibrational averaging of the molecular geometry.

IV. Discussion

A. Vibrational Predissociation/Relaxation Dynamics

Certainly one of the most intriguing results to come of these high-resolution IR studies *is the fact that structured spectra exist at all* in the near-IR for these vibrationally excited, weakly bound complexes! The intramolecular vibrational energies in the subunits typically are many times the dissociation limit of the complex; hence the upper states are metastable with respect to vibrational[16] (and in some cases rotational)[52,64,65] predissociation. Coupling between strongly bound, high-frequency (intramolecular) modes and dissociating, low-frequency (intermolecular) modes can promote vibrational energy redistribution within the complex, which eventually excites the weak intermolecular bond to the point of breaking. Quantum mechanically, these vibrational couplings cause a mixing of the zeroth-order excited state with the continuum, thereby distributing oscillator strength for the transition over a continuous range of nearby frequencies (i.e., line broadening). The width of these broadened absorptions is a measure of the strength of these couplings, as well as of the time scale of this vibrational energy flow.

If the coupling is independent of internal energy over the width of broadened lines, this problem is isomorphic with that of radiative coupling of an excited state with the continuum, which was solved by Weisskopf and Wigner[225] and for which a Lorentzian absorption line shape and a single-exponential decay of the upper state population can be derived.[225] The relationship between *FWHM* of the Lorentzian line shape and the $1/e$ lifetime of the upper state *probability* is given by

$$\tau_{VP}\ (s) = \frac{1}{2\pi\Delta\nu_{FWHM(Hz)}} \qquad (4.1)$$

There has been a discrepancy of a factor of 2 in the literature[60,61,73,117] over the expression used to obtain lifetime estimates, but which seems to be largely resolved.[129,218] In light of the rapid progress in direct time probing[226] of van der Waals vibrational predissociation phenomena, it is particularly important to have a consistent and quantitatively correct measure of these predissociation/relaxation lifetimes from spectroscopic data. To avoid perpetuating these inconsistencies in the literature, all measurements of predissociation widths in this review have been reported as the original experimental values of FWHM line widths, and any conversions to lifetimes have been made via the correct eq 4.1.

In order for rotational structure in the spectrum to be resolvable, the excited states need to survive for at least a time comparable to end-over-end rotational periods in the complex. Given the roughly 10^4-fold difference between typical rotational and intramolecular vibrational periods, therefore, it is by no means obvious that rotational structure in an IR spectrum of weakly bound complexes would ever be observable. Indeed, the laser-induced fluorescence work of Levy and co-workers[17] on I_2–inert gases indicated relatively efficient coupling of I_2 vibration to the dissociation coordinate, and there existed a large body of data on IR predissociation of ethylene complexes with a line-tunable CO_2 laser that suggested 1–20-cm^{-1} broad, structureless vibrational absorption bands,[24,25] though recent data have demonstrated highly structured absorptions in ethylene dimers.[29,30] Theoretical calculations, on the other hand, have made predictions for various models[16,180,227] of vibrational predissociation lifetimes that varied from picoseconds to minutes! With the roughly 80 vibrationally and rotationally resolved bands of complexes assigned thus far (see Figures 1 and 2), we can see experimental values for homogeneous line widths that range from $<1.8 \times 10^{-8}$ cm^{-1} ($\tau_{VP} > 3 \times 10^{-4}$ s) inferred for ν_1 excited Ar–HF[116] to on the order of 0.5 cm^{-1} ($\tau_{VP} \gtrsim 10$ ps) observed for the ν_2 mode of linear HCN trimer.[171] This 30-million-fold dynamic range is likely to be even larger, but for line widths above roughly 0.1 cm^{-1} rotational structure begins to be lost, and at the other extreme, collision-free lifetimes $\gtrsim$1 ms are simply difficult to observe in apparatus of finite size. Nonetheless even the 0.5-cm^{-1} predissociation line widths observed in vibrationally excited HCN trimer still correspond to over 1000 vibrations of the HCN subunit. It is clear therefore that vibrational energy flow from the initially excited mode into intermolecular stretching coordinates can be quite inefficient, and certainly must be for any weakly bound complexes that exhibit rotationally resolved spectra at energies above the dissociation limit.

One important issue that must be addressed in any direct inference of predissociation lifetime from experimentally determined homogeneous line widths is the possible contribution to the line width from intramolecular vibrational relaxation (IVR).[228] Simply stated, for a molecule with sufficient state density, internal vibrations of the complex can in principle act as a local "bath" of states into which the initial excitation can relax but without immediately depositing enough

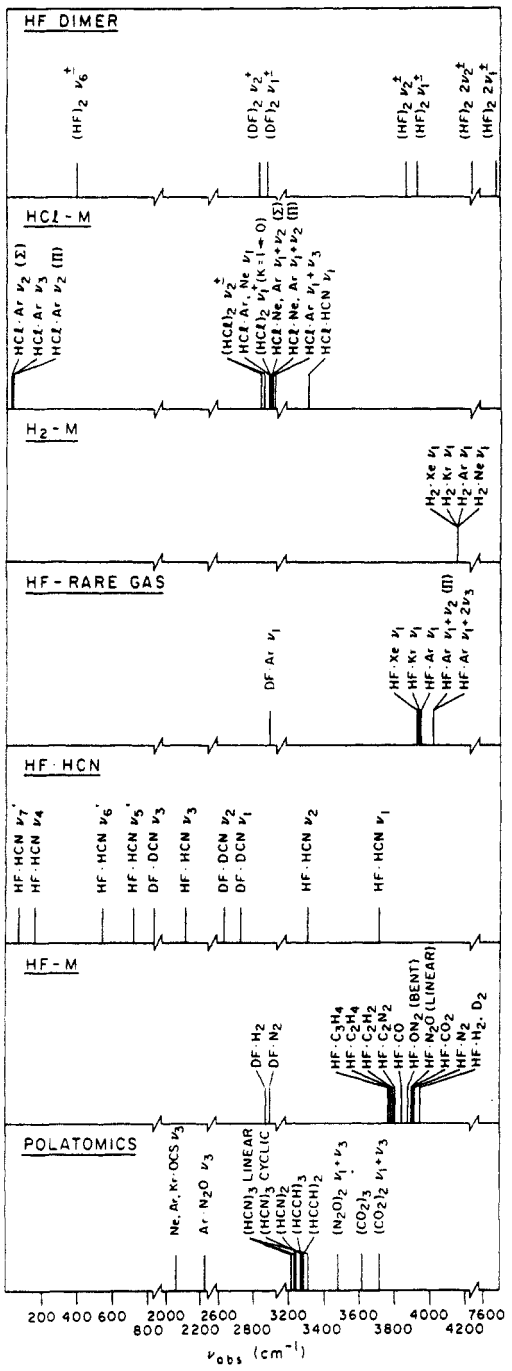

Figure 2. Graphical summary of the vibrational origins of all complexes investigated via high-resolution, rotationally resolved, and assigned infrared spectroscopic methods. Many vibrational hot bands, isotope, and K subband origins have been suppressed for clarity. Note the several breaks in the frequency axis.

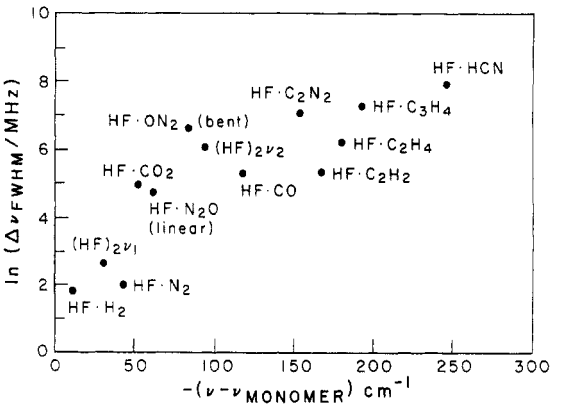

Figure 3. Semilogarithmic plot of homogeneous line width (FWHM in MHz) measured via high-resolution infrared spectroscopy versus red shift of the vibrational origin from the monomer absorption frequency. References to the data can be found in Tables I–VII.

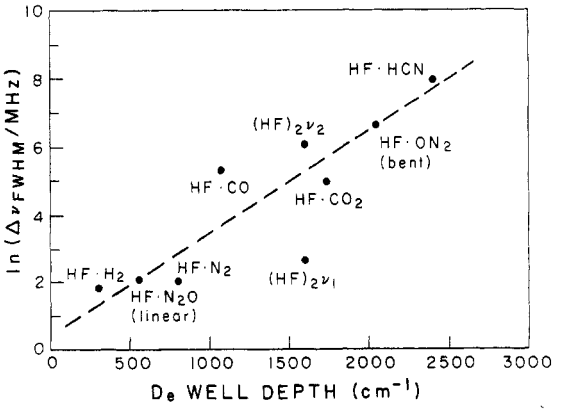

Figure 4. Semilogarithmic plot of homogeneous line width (FWHM in MHz) measured via high-resolution infrared spectroscopy versus well depths for several HF-containing complexes. For consistency, these well depths are all taken from ab initio theoretical calculations cited in Tables I–VII, with the exception of HF dimer, which is an experimental value of Pine and Howard.[62] The dashed line is intended only to guide the eye and underscore the nearly exponential correlation between homogeneous line width and well depth.

energy into a intermolecular mode to dissociate. Spectroscopically, these vibrational couplings to other metastable vibrations in the complex can produce densely spaced lines that overlap within their individual predissociation line widths and thus yield a much broader, homogeneous line width from which one might underestimate the predissociation lifetime. Strictly speaking, therefore, the collision-free line widths represent a measurement of the combined "predissociation/relaxation" pathway, and are intended as such in this review. However, as pointed out by several workers,[119,128,129] the total state density in many of the smaller complexes is not large enough to rationalize unstructured, Lorentzian lines without directly invoking the continuum. Furthermore, in the bolometric[21,28] and mass spectrometric based studies,[10,20,24,25] the depletion signals indicate that laser-induced predissociation of the complexes away from the beam occurs at least before 10^{-3} s (Ar–HF being the notable exception[116]). This issue is best resolved by direct measurements in the time domain such as has been initiated by Casassa et al.[226] for study of vibrational predissociation of NO dimer. It would be particularly interesting to have direct comparisons between predissociation lifetime and line width measurements on the same molecular system, in order to determine the importance of radiationless channels such as IVR which may not lead promptly to dissociation.

In the meantime, there already exists a significant data set on predissociation/relaxation line widths in HF-containing complexes with which to search for simple trends. Indeed, the data in Tables I–VII indicate a strong correlation of the observed line widths on both the ground-state well depth and red shift of the HF stretch from the free monomer value. An approximately exponential correlation is suggested by the

semilogarithmic plots of $\Delta\nu_{FWHM}$ versus red shift and well depth in Figures 3 and 4, respectively. Although a correlation does not necessarily imply a causal relationship, this trend is physically plausible if the magnitude of the vibrational mode coupling responsible for predissociation scales with the overall strength of interaction between the substituents. Even this approximate correlation clearly must break down in the limit of sufficiently strong binding to render dissociation from the vibrationally excited state an endothermic channel. It also fails qualitatively in a prediction of the $\gtrsim$0.3-ms lifetimes for ν_1 excited Ar–HF. Nonetheless, the enormous dynamic range of predissociation/relaxation behavior indicates an extreme sensitivity to small changes in the molecular potential energy surfaces.

There have been many theoretical models[16,53,55,158,170,180] proposed to predict trends in vibrational predissociation behavior. A common feature of may of these theories is that transitions between bound and dissociative states are strongly enhanced by resonances that require little excess energy deposited into relative translation of the fragments. This would account for the exceedingly long lifetimes of the triatomic inert gas–HF complexes, in which high rotation of the HF fragment is the only energetically accessible channel for minimizing translation energy. Indeed, full close-coupled calculations on vibrational predissociation in H_2–Ar[53,55] and Ar–HCl[229] do indicate a peaking of the final J states of H_2 and HCl, respectively, in the highest accessible rotational channels. In larger than triatomic systems there exist multiple rotational and vibrational degrees of freedom, and the density of near-resonant (and hence possibly strongly favored) dissociation pathways grows correspondingly. This is certainly evident with the steady increase in predissociation/relaxation rates in complexes of HF with hydrocarbons (see Table VI). However, the significant difference between N_2–HF[119] and OC–HF[211] line widths, for example, is difficult to explain in light of the similarity of bonding strengths, vibrational frequencies, rotational constants, etc.

The importance of specific vibrational couplings is not considered in such a simple resonance picture, and yet the dramatic effects of these couplings are manifested clearly in the strongly vibrational mode dependent line widths observed for HF dimer ($\Delta\nu_1$ = 13.4 MHz, $\Delta\nu_2$ = 408 MHz),[60,61,117] HCN–HF ($\Delta\nu_1$ = 2722 MHz, $\Delta\nu_2$ = 11.8 MHz, $\Delta\nu_3$ = 558 MHz)[73,209] and HCN trimer ($\Delta\nu_1 \lesssim 1$ MHz, $\Delta\nu_2 \approx$ 15 000 MHz, $\Delta\nu_3$ = 56 MHz).[171] Additional data from direct time-resolved studies of vibrationally excited NO dimer (τ_{ν_1} = 880 ps, τ_{ν_4} = 39 ps) also indicate a mode-specific predissociation pathway.[226] In each of these systems the behavior appears to be nonstatistical; i.e., the predissociation rates do not scale monotonically with excess vibrational energy. This non-RRKM behavior indicates that dynamical rather than purely statistical effects are important and thus require a more sophisticated consideration of the potential energy surface.

It can defensibly be argued that vibrational mode–mode coupling in complexes is so weak that small differences in the potential surface translate into large differences in predissociation rates. If this is the case, predissociation trends in isotopically substituted complexes should help identify the key dynamical effects more readily than comparison between different complexes. In HF dimer, for example, the line widths for the ν_2 H-bonded HF stretching vibration decrease below the Doppler resolution limit for DF dimer and the mixed HF–DF and DF–HF species.[60,61] This behavior is inconsistent with energy[16] or momentum gap[227] laws proposed to explain the extremely slow predissociation in triatomics. If channels that minimize translational energy in the fragments predissociate preferentially, a more likely interpretation is that more rotational quanta are required to achieve a near resonance for DF ($B_{rot} \approx 10$ cm^{-1}) than HF ($B_{rot} \approx 20$ cm^{-1}) containing complexes. This " quantum gap" perspective may also help explain the much narrower line widths in HCl dimer spectra,[63,160] since near-resonant dissociation would also require more rotational quanta in the HCl fragment ($B_{rot} \approx 10$ cm^{-1}). Similarly, in DCN–DF complexes,[77] the line widths for the DF and CN stretching modes are narrower than in the corresponding HCN–HF vibrations, though the number of vibrational channels energetically accessible in the outgoing substituents makes a clear interpretation more difficult. Further isotopic substitution studies in HF/DF, HCl/DCl, and HCN/DCN systems would be very useful in testing these dynamical models in more detail.

B. Intermolecular Bend–Stretch Coupling

Vibrational predissociation occurs via direct or indirect coupling of the initially excited mode with the intermolecular stretch coordinate. It is therefore useful to consider in detail what spectroscopic evidence the data provides for the magnitudes of these mode–mode couplings.

A numerically exact treatment of the rovibrational Schroedinger equation even for a two-dimensional, "ball and stick" model of a van der Waals triatomic requires solution of close-coupled equations for the stretching and bending degrees of freedom, the difficulty of which substantially restricts a least-squares fitting of experimental data to a potential surface. Toward that end, an approximate (BOARS) decoupling of the stretch and bend degrees of freedom was proposed by Holmgren et al.,[151] whereby an effective one-dimensional radial potential was constructed from the full potential surface by solving the angular Hamiltonian parametrically as a function of internuclear distance. Hutson and Howard[152] later used refinement of the BOARS method (CBO) which perturbatively includes first-order radial–angular couplings to least-squares fit two-dimensional potential surfaces from microwave, line broadening, virial coefficient, and scattering data for hydrogen halide–inert gas complexes. These semiempirical surfaces[191-193] have proven remarkably successful in predicting energies of excited van der Waals vibrational states and thereby stimulating further experimental effort.

Recent infrared spectroscopic data suggest that there is a significant degree of coupling between inter- and intramolecular modes in hydrogen halide complexes. In HCN–HF,[68] for example, there is a +2% increase in B upon ν_1 excitation, resulting from a deepening of the radial well. Indeed, a shortening of the intermolecular bond is observed upon HF excitation in every HF-containing complex studied thus far in the infrared. Additionally, there is evidence for interaction of bend

and stretch degrees of freedom in the spectra that may necessitate explicit inclusion of angular–radial couplings in the analysis. Increase in the anisotropy of the angular HF potential in several HF complexes is evidenced by the increased dipole moment,[116,119,187] and hence more directional "pointing" of the HF in the upper state. A direct vibrational coupling of bend with the intermolecular stretch is demonstrated by the increase in the vibrationally averaged separation upon excitation of perpendicular bending modes.[64,126] Quantitative evidence for these stretch–bend couplings in rotating Ar–HF complexes has been obtained via analysis of Coriolis crossing between the ν_2 (Π) perpendicular bend and the $2\nu_3$ (Σ) overtone of the van der Waals stretch vibration.[126] Resonant crossings of coupled vibrational states also have been observed as isolated perturbations and analyzed in OC–HF[211] and HCN–HF[78] complexes, though identification of the perturbing vibration is not as straightforward in these polyatomic systems. Interestingly, the line widths observed at the crossing in the OC–HF system differ dramatically from the unperturbed transitions,[211] indicating that these intramolecular vibrational couplings can indeed influence predissociation/relaxation dynamics.

Coupling between the intermolecular bending and stretching modes in Ar–HCl is particularly well demonstrated in the far- and near-infrared data of Robinson et al.[139-141] and Lovejoy and Nesbitt,[201] respectively. For both HCl $\nu_1 = 0$ and 1 complexes, the van der Waals ν_3 stretch vibration acquires roughly 20% of the oscillator strength of either Π or Σ bending vibration. This must result largely from a coupling of radial with angular motion, since one anticipates little dipole transition moment associated directly with purely radial motion of the Ar and HCl centers of mass. Indeed, by analysis of the high J rotational states ($J \lesssim 30$), Lovejoy and Nesbitt[201] have observed considerable Coriolis coupling between the perpendicular bend and both the parallel bend and stretch modes.

C. Equilibrium and Vibrationally Averaged Structures

One key focus of studies of weakly bound complexes has been a more complete characterization of the potential energy surface, since such a surface completely governs the collisional and "half-collisional" dynamics of the subunits. The equilibrium structure of a complex is determined by the absolute minimum in this surface. However, by virtue of shalow potential wells along a particular coordinate or large zero-point motion of light atoms, the ground-state wave function may sample configurations significantly away from the equilibrium geometry. This large-amplitude motion is more the rule than exception in weakly bound complexes, particularly for hydrogen- or deuterium-containing species. Nevertheless, it appears an incurable (and perhaps not completely undesirable) trend in the literature to focus on either an equilibrium or vibrationally averaged geometry as a convenient, single-parameter characterization of this multidimensional surface and furthermore to develop simple unifying concepts that can reliably predict these structural trends. It is both in support and in defiance of these traditional concepts that the recent infrared data have made significant contributions.

The MBER rotational and hyperfine studies of van der Waals complexes[10,11] has fostered lively discussion[230,231] about the relative importance of physical (i.e., electrostatic) and chemical (i.e., charge donation) interactions in determining an equilibrium structure. In the former description,[205,230] point multipoles, distributed on the molecular framework, can be used to model the isolated electrostatic properties of the subunits obtained via experiment or independent ab initio calculations. An approximate surface can then be generated from a sum of these electrostatic terms plus repulsive terms chosen to model hard-core interactions (e.g., van der Waals radii). The potential advantage of such an approach is that the electrostatic properties of the subunits do not need to be recalculated for every complex. Proponents of chemically mediated binding in complexes argue that the charge-exchange interactions between the highest occupied and lowest unoccupied molecular orbitals (HOMO–LUMO)[231] are important in determining equilibrium structures and that the quantitative details of such "incipient chemistry" require a full ab initio calculation on the combined subunits. Such full ab initio calculations unquestionably can determine the correct answer but at some loss of an intuitive physical picture of the interactions; the key issue is whether the simpler, electrostatic description captures enough of the relevant physics to explain or, even better, predict experimental results satisfactorily.

Several recent examples from rotationally resolved infrared spectroscopy suggest that this may be the case. The slipped-parallel equilibrium structures of CO_2 dimers[118] inferred from high-resolution infrared spectroscopy are in good quantitative agreement with the predictions of a quadrupole–quadrupole electrostatic plus hard-sphere potential.[11,118,161] Similar calculations have been performed by Fraser et al.[120] to obtain impressive agreement with the planar structure of CO_2 trimer as well. The equilibrium structure of N_2O dimer predicted from an electrostatic plus Lennard-Jones atom–atom potential also agrees nicely with the infrared data.[167] The slipped-parallel geometry of HCCH dimer[162] appears to be similarly well characterized by electrostatic calculations.

It is clear from observed enhancements of dipole moments measured upon complexation, however, that induction effects must play an important role in the interaction. The electrostatic treatment can be refined by inclusion of both multipoles and multipolar polarizabilities from high-quality ab initio calculations on the monomer.[173,185,196,197,202,204] These methods have been exploited to predict frequency shifts of the intramolecular vibrations, equilibrium geometries, and induced dipole moments for several complexes of HF that are in fair agreement with experiment. A particular success of these methods is in the prediction of an extremely flat intermolecular bending potential for OCO–HF,[205] which is consistent with large-amplitude, low-frequency bending motion of the CO_2 around a linear equilibrium geometry.[129] A much tighter bending potential is predicted for N_2–HF,[202] and indeed this is observed to be a much more rigid, linear complex.[128] It is worth noting, of course, that one could arrive at the same qualitative conclusion via the more chemically based concepts of Lewis acid–base interactions between HF and the ni-

trogen and oxygen terminus, which have collinear (sp) and off-axis (sp^2) hybridized lone-pair electron density, respectively. Some[208] but not all electrostatic[205,206] calculations have correctly predicted the existence of multiple minima in the N_2O–HF potential, and hence the possibility for geometric isomers.

There appear to be several examples provided by IR spectroscopy, however, which are not in agreement with predictions from electrostatic theories. The magnitude of dipole moment enhancement upon vibrational excitation in HF–hydrocarbon complexes, for example, does not appear to be explained by simply electrostatic and induction effects.[202] There also appear to be considerable discrepancies between electrostatic calculations[173] and IR–microwave experiments[100-102] for the equilibrium structure and dipole moment of NH_3 dimers. One should hasten to point out, however, that several ab initio calculations[136-138] on NH_3 dimer have similarly failed to predict the observed behavior. In light of the importance of establishing the limits of credibility of these approximate theories, it would be extremely useful to have more rotationally resolved data on NH_3 dimer in both the near- and far-IR.

While the above cases indicate how infrared experiments have been quite useful in furnishing structural information on the *equilibrium* geometry of complexes, the real advantage in the infrared is in sampling parts of the potential surface *away from equilibrium*, and in particular probing the large-amplitude motion associated with the low-frequency intermolecular vibrations. Previously, the degree of large-amplitude motion had been inferred from precise measurements of molecule-fixed projections of multipole moments, nuclear spin hyperfine structure,[10,11] and centrifugal distortion effects in the *ground* vibrational state. With the recent intermolecular vibrational information from hot bands and combination bands in the near-IR, as well as direct excitation methods in the far-IR, the methods are at hand for probing directly the topology of the intermolecular potential surface.

The evidence accumulated thus far suggests that molecular complexes can vary dramatically in their degree of intermolecular rigidity. N_2–HF[128] and HCN–HF,[75,76] for example, exhibit relatively stiff bending potentials as derived from measurements of the low-frequency bending vibrations. On the other hand, OCO–HF complexes[129] exhibit bending frequencies an order of magnitude lower. The data are consistent with large-amplitude motion in the CO_2 subunit around a linear geometry. Electrostatic calculations on CO_2,[163] N_2O,[113] and HCCH[161] dimers indicate the possibility of multiple structures and moderate-energy pathways between these structures. The direct observation of such geometric isomers in N_2O–HF[130,209] and HCN trimer[171] demonstrates clearly that multiple minima of comparable binding energy can exist in a potential surface. Isomerization between these structures involves motion along intermolecular bending coordinates. With excitation of the bending vibration, therefore, one can anticipate dramatic quantum state dependent changes in the effective vibrationally averaged geometry of the complex. For example, in Ar–HCl the wave function for the parallel bend excited state significantly samples the secondary minimum in the potential at the inverted Ar–ClH configuration.[192] Similarly, a T-shaped *equilibrium* structure of H_2–HF is correctly predicted from electrostatic quadrupole–dipole and quadrupole–quadrupole interactions,[185] but large-amplitude hindered rotor motion in the H_2 angular coordinate yields a nearly isotropic H_2 angular distribution for the ground-state (para) complexes, while yielding a more localized T-shaped geometry only for the excited (ortho) complexes.

These considerations suggest that vibrationally averaged information obtained only from states unexcited in the low-frequency intermolecular modes may be concealing important topological features of the potential surface. This could be especially insidious for jet-cooled studies in the near-infrared, where the upper state is typically excited to an intramolecular vibration, but the low temperatures attained in a supersonic jet dramatically limit the range of lower J, K, and intermolecular vibrational states observed. This has been tested recently[232] in model potential systems representing two extreme limits of floppy motion in triatomics: (1) a square-well ABC bending potential (i.e., a free "hinge") and (2) hindered internal rotation of BC in the complex (i.e., a "pinwheel"). Full quantum calculations for the rovibrational states in the *floppy* limit predict spectra that are exceedingly difficult to distinguish from a *highly rigid* limit for an ABC molecule of considerably different geometry. This underscores the importance of encouraging a variety of research efforts in the far-IR, near-IR, and microwave. Particularly relevant will be studies of multiple vibrational, J, K levels, hyperfine structure, multipolar moments, and isotopically substituted complexes in order to infer correctly the precise topology of the intermolecular potential surface.

V. Summary

The field of high-resolution infrared spectroscopy of weakly bound complexes has enjoyed, by virtue of the development of several experimental techniques with requisite sensitivity and spectral resolution, an explosive growth in the past 5 years. The spectroscopic information on vibrational states of complexes offers our first detailed glimpses of excited, but bound regions of the intermolecular potential energy surface, thereby helping bridge the gap between microwave studies of the ground state, and bulk transport, pressure broadening, and molecular beam studies of the continuum states. These methods now allow us to address in great detail interesting dynamical issues such as vibrational predissociation/relaxation in metastable vibrational states via spectral line-broadening studies. Vibrationally averaged structures in these complexes are obtained that can rigorously test the best available theoretical models or calculations of bonding in weakly attractive systems. Detailed analysis of the rovibrational eigenvalues in floppy molecular systems with large-amplitude motion allows one to probe the eigenstructure of highly coupled vibrations and rotations.

The wealth of new data provided on complexes previously studied in the microwave underscores the synergistic advantages for multiple efforts on the same molecular systems. For example, the combination of microwave, far-infrared, and near-infrared investigations of Ar–HCl have provided an unprecedented set of data for fitting of the full potential energy surface.

Of comparable importance is the need for information from both ultracold pinhole (1–2 K) and slit (5–30 K) expansions as well as from the cooled, but much warmer equilibrium White cells, in order to obtain spectroscopic data over the widest possible range of vibrational and rotational quantum states. The supersonic jet studies may prove most useful in the initial detection and spectral characterization of the complexes, but the data from much warmer systems will probably be necessary to investigate more of the multiply vibrationally excited states via thermally populated hot bands, as well as to investigate rotational energy levels near the dissociation limit. Also useful are isotopic substitution studies to elucidate the effects of wide-amplitude vibrational averaging that may be masked by observation solely of levels populated in a supersonic jet. The central role of ab initio, electrostatic, and semiempirical theoretical studies in providing the necessary guidance for experimental efforts is absolutely crucial and cannot be underestimated.

Directions for future growth in the field are manifold. The observation of several trimers with rotationally resolvable and assignable structure as well as the identification of likely candidates for tetramer species bodes well for the extension of these high-resolution methods into even larger molecular clusters. The data thus far even on trimers have elucidated some intriguing comparisons with condensed-phase crystal structure. Particularly in these larger clusters, it seems likely that multiple isomeric configurtions will continue to be discovered. Double-resonance techniques may prove a necessary and powerful extension of these methods for assigning even jet-cooled spectra of mixtures of these clusters.

The vibrational predissociation studies in the infrared have indicated some fascinating nonstatistical behaviors that would be important to probe in the final state distributions. There are clear theoretical predictions that indicate that high rotational excitation in the products is expected. Methods for state-resolved detection of molecular fragments are already feasible with LIF or MPI detection and therefore should make possible time-resolved dynamical studies of photofragmentation. The experiments promise to be quite hard, but the dynamical possibilities commensurately rich.

Much progress has been made in the past years on ab initio calculations of potential energy surfaces. The precise calculation of surfaces at the level of accuracy required to predict detailed spectroscopic behavior in weakly bound complexes is still quite difficult except for the simplest of systems. It would seem appropriate, therefore, to establish benchmark complexes that represent a compromise between experimentally feasibility and fewest number of electrons (e.g., Ne–HF), for direct comparison between state-of-the-art ab initio theory and high-resolution experimental results.

The importance of semiempirical methods for fitting potential energy surfaces to high-resolution data would also be hard to overstate. At present there is a rapidly growing surplus of data that have been more or less accurately parametrized by conventional spectroscopic analysis but that have not been exploited beyond a simple characterization of vibrationally averaged geometries. It appears an extremely opportune and productive point in the field's growth for continued synergism between theoretical and experimental efforts in order to generate the best possible intermolecular potentials and thereby to stimulate further dynamical and spectroscopic studies of weakly bound molecular complexes.

Acknowledgments. This work has been supported by grants from the National Science Foundation (Grants CHE86-05970 and PHY86-04504), the Petroleum Research Fund, administered by the American Chemical Society, and Research Corporation. Further support from the Henry and Camille Dreyfus Foundation and the Alfred P. Sloan Foundation are gratefully acknowledged. I also thank the members of my group for their patience during the period of writing of this review.

References

(1) Weber, A., Ed. *Structure and Dynamics of Weakly Bound Molecular Complexes*; NATO Advanced Scientific Institute Series C 212, 1987.
(2) Truhlar, D. G., Ed. *Resonances in Electron–Molecule Scattering, van der Waals Complexes and Reactive Chemical Dynamics*; ACS Symposium Series 263; American Chemical Society: Washington, DC, 1984.
(3) Lambert, J. D. *Vibrational and Rotational Relaxation in Gases*; Clarendon: Oxford, 1977.
(4) Yardley, J. T. *Introduction to Molecular Energy Transfer*; Academic: New York, 1980.
(5) Leone, S. R. "A Compilation of Rate Coefficients for Vibrational Energy Transfer Involving the Hydrogen Halides". *J. Phys. Chem. Ref. Data* **1981**, *11*, 953.
(6) Leone, S. R. *Adv. Chem. Phys.* **1982**, *50*, 255.
(7) Pine, A. S.; Looney, J. P. *J. Mol. Spectrosc.* **1987**, *122*, 41.
(8) Pimentel, G. C.; McClellan, A. L. *The Hydrogen Bond*; W. H. Freeman: San Francisco, 1960.
(9) Hirschfelder, J. O.; Curtiss, C. F.; Bird, R. B. *Molecular Theory of Gases and Liquids*; Wiley: New York, 1954.
(10) Muenter, J. S. *Structure and Dynamics of Weakly Bound Molecular Complexes*; Weber, A., Ed.; NATO Advanced Scientific Institute Series C 212, 1987, p 3.
(11) Legon, A. C. *Structure and Dynamics of Weakly Bound Molecular Complexes*; Weber, A., Ed.; NATO Advanced Scientific Institute Series C 212, 1987, p 23.
(12) Levy, D. H. *Adv. Chem. Phys.* **1981**, *47*, 323.
(13) Legon, A. C.; Millen, D. J.; Rogers, S. C. *Proc. R. Soc. London, Ser. A* **1980**, *370*, 213.
(14) Kisiel, Z.; Legon, A. C.; Millen, D. J. *Proc. R. Soc. London, Ser. A* **1982**, *381*, 419.
(15) Levy, D. H. *Annu. Rev. Phys. Chem.* **1980**, *31*, 197.
(16) Beswick, J. A.; Jortner, J. *Adv. Chem. Phys.* **1981**, *47*, 363.
(17) Kenny, J. E.; Johnson, K. E.; Sharfin, W.; Levy, D. H. *J. Chem. Phys.* **1980**, *72*, 1109.
(18) Brinza, D. E.; Swartz, B. A.; Western, C. M.; Janda, K. C. *J. Chem. Phys.* **1983**, *79*, 1541.
(19) Vernon, M. F.; Lisy, J. M.; Kwok, H. S.; Krajnovich, D. J.; Tramer, A.; Shen, Y. R.; Lee, Y. T. *J. Phys. Chem.* **1981**, *85*, 3327.
(20) Vernon, M. F.; Krajnovich, D. J.; Kowk, H. S.; Lisy, J. M.; Shen, Y. R.; Lee, Y. T. *J. Chem. Phys.* **1982**, *77*, 47.
(21) Gough, T. E.; Miller, R. E.; Scoles, G. *J. Chem. Phys.* **1978**, *69*, 1588.
(22) Liu, W.-L.; Kolenbrander, K. D.; Lisy, J. M. *Chem. Phys. Lett.* **1984**, *112*, 585.
(23) Kolenbrander, K. D.; Lisy, J. L. *J. Chem. Phys.* **1986**, *85*, 2463.
(24) Casassa, M. P.; Western, C. M.; Celli, F. G.; Brinza, D. E.; Janda, K. C. *J. Chem. Phys.* **1983**, *79*, 3227.
(25) Howard, M. J.; Burdenski, S.; Giese, C. F.; Gentry, W. R. *J. Chem. Phys.* **1984**, *80*, 4137.
(26) Fischer, G.; Miller, R. E.; Vohralik, P. F.; Watts, R. O. *J. Chem. Phys.* **1985**, *83*, 1471.
(27) Geraedts, J.; Setiadi, S.; Stolte, S.; Reuss, J. *Chem. Phys. Lett.* **1981**, *78*, 277.
(28) Miller, R. E. *J. Phys. Chem.* **1986**, *90*, 3301.
(29) Snels, M.; Fantoni, R.; Zen, M.; Stolte, S.; Reuss, J. *Chem. Phys. Lett.* **1986**, *124*, 1.
(30) Baldwin, K. G. H.; Watts, R. O. *Chem. Phys. Lett.* **1986**, *129*, 237.
(31) Stepanov, B. I. *Nature (London)* **1946**, *157*, 808.
(32) Bertie, J. E.; Millen, D. J. *J. Chem. Soc.* **1965**, 497.
(33) Rank, D. H.; Rao, B. S.; Wiggins, T. A. *J. Chem. Phys.* **1962**, *37*, 2511.

(34) Rank, D. H.; Sitaram, P.; Glickman, W. A.; Wiggins, T. A. *J. Chem. Phys.* **1963**, *59*, 2673.
(35) Vodar, B.; Vu, H. *J. Quant. Spectrosc. Radiat. Transfer* **1963**, *3*, 397.
(36) Hyde, G. E.; Hornig, D. F. *J. Chem. Phys.* **1952**, *20*, 647.
(37) Jones, W. J.; Seel, R. M.; Sheppard, N. *Spectrochim. Acta, Part A* **1969**, *25*, 385.
(38) Mannik, L.; Stryland, J. C.; Welsh, H. L. *Can. J. Phys.* **1971**, *49*, 3056.
(39) Pendley, R. D.; Ewing, G. E. *J. Chem. Phys.* **1983**, *78*, 3531.
(40) Pine, A. S. *Philos. Trans. R. Soc. London, A* **1982**, *307*, 481.
(41) Patel, C. K. N.; Tam, A. C. *Rev. Mod. Phys.* **1981**, *53*, 517.
(42) Miller, R. E. *Molecular Beams*; Scoles, G., Ed.; Oxford University Press: Oxford, in press.
(43) Ray, D.; Robinson, R. L.; Gwo, D.-H.; Saykally, R. J. *J. Chem. Phys.* **1986**, *84*, 1171.
(44) McQuarrie, D. A. *Statistical Mechanics*; Harper: New York, 1976.
(45) Gribov, L. A.; Smirnov, V. N. *Sov. Phys. Usp.* **1962**, *4*, 919.
(46) Nesbitt, D. J.; Petek, H.; Gudeman, C. S.; Moore, C. B.; Saykally, R. J. *J. Chem. Phys.* **1984**, *81*, 5281.
(47) Watanabe, A.; Welsh, H. L. *Phys. Rev. Lett.* **1964**, *13*, 810.
(48) Kudian, A. K.; Welsh, H. L.; Watanabe, A. *J. Chem. Phys.* **1965**, *43*, 3397.
(49) Kudian, A. K.; Welsh, H. L. *Can. J. Phys.* **1971**, *49*, 230.
(50) McKellar, A. R. W.; Welsh, H. L. *J. Chem. Phys.* **1971**, *55*, 595.
(51) McKellar, A. R. W.; Welsh, H. L. *Can. J. Phys.* **1972**, *50*, 1458.
(52) McKellar, A. R. W. *Faraday Discuss. Chem. Soc.* **1982**, *73*, 89.
(53) LeRoy, R. J.; Corey, G. C.; Hutson, J. M. *Faraday Discuss. Chem. Soc.* **1982**, *73*, 339.
(54) Ashton, C. J.; Child, M. S.; Hutson, J. M. *J. Chem. Phys.* **1983**, *78*, 4025.
(55) Hutson, J. M.; Ashton, C. J.; LeRoy, R. J. *J. Phys. Chem.* **1983**, *87*, 2713.
(56) Hutson, J. M.; LeRoy, R. J. *J. Chem. Phys.* **1983**, *78*, 4040.
(57) LeRoy, R. J. *Resonances in Electron–Molecule Scattering, van der Waals Complexes and Reactive Chemical Dynamics*; Truhlar, D. G., Ed.; ACS Symposium Series 263; American Chemical Society: Washington, DC, 1984; p 231.
(58) Legon, A. C.; Millen, D. J. *Faraday Discuss. Chem. Soc.* **1982**, *73*, 71.
(59) Pine, A. S. *J. Opt. Soc. Am.* **1974**, *64*, 1683.
(60) Pine, A. S.; Lafferty, W. J. *J. Chem. Phys.* **1983**, *78*, 2154.
(61) Pine, A. S.; Lafferty, W. J.; Howard, B. J. *J. Chem. Phys.* **1984**, *81*, 2939.
(62) Pine, A. S.; Howard, B. J. *J. Chem. Phys.* **1986**, *84*, 590.
(63) Ohashi, N.; Pine, A. S. *J. Chem. Phys.* **1984**, *81*, 73.
(64) Fraser, G. T.; Pine, A. S. *J. Chem. Phys.* **1986**, *85*, 2502.
(65) Howard, B. J.; Pine, A. S. *Chem. Phys. Lett.* **1985**, *122*, 1.
(66) Wang, F. M.; Iqbal, K.; Kraft, H.-G.; Luckstead, M.; Eue, W. C.; Bevan, J. W. *Can. J. Chem.* **1982**, *60*, 1969.
(67) Kyrö, E. K.; Chaghervand, P. S.; McMillan, K.; Eliades, M.; Danzeiser, D. A.; Bevan, J. W. *J. Chem. Phys.* **1983**, *79*, 78.
(68) Kyrö, E.; Warren, R.; McMillan, K.; Eliades, M.; Danzeiser, D.; Chaghervand, P. S.; Lieb, S. G.; Bevan, J. W. *J. Chem. Phys.* **1983**, *78*, 5881.
(69) Kyrö, E. K.; Eliades, M.; Gallegos, A. M.; Chaghervand, P. S.; Bevan, J. W. *J. Chem. Phys.* **1986**, *85*, 1283.
(70) Pollock, C. R.; Kaspar, J.; Ernst, G. K.; Ernst, W. E.; Blit, S.; Tittel, F. D. *App. Opt.* **1979**, *18*, 1907.
(71) Campbell, E. J., private communication.
(72) Bevan, J. W.; Martineau, B.; Sandorfy, C. *Can. J. Chem.* **1979**, *57*, 1341.
(73) Wofford, B. A.; Bevan, J. W.; Olson, W. B.; Lafferty, W. T. *J. Chem. Phys.* **1985**, *83*, 6188.
(74) Jackson, M. W.; Wofford, B. A.; Bevan, J. W.; Olson, W. B.; Lafferty, W. J. *J. Chem. Phys.* **1986**, *85*, 2401.
(75) Wofford, B. A.; Jackson, M. W.; Bevan, J. W.; Olson, W. B.; Lafferty, W. J. *J. Chem. Phys.* **1986**, *84*, 6115.
(76) Wofford, B. A.; Bevan, J. W.; Olson, W. B.; Lafferty, W. J. *Chem. Phys. Lett.* **1986**, *124*, 579.
(77) Jackson, M. W.; Wofford, B. A.; Bevan, J. W. *J. Chem. Phys.* **1987**, *86*, 2518.
(78) Bender, D.; Eliades, M.; Danzeiser, D. A.; Jackson, M. W.; Bevan, J. W. *J. Chem. Phys.* **1987**, *86*, 1225.
(79) Bender, D.; Eliades, M.; Danzeiser, D. A.; Fry, E. S.; Bevan, J. W. *Chem. Phys. Lett.* **1986**, *131*, 134.
(80) Wofford, B. A.; Bevan, J. W.; Olson, W. B.; Lafferty, W. J. *J. Chem. Phys.* **1986**, *85*, 105.
(81) Von Puttkamer, K.; Quack, M. *Mol. Phys.* **1987**, *62*, 1047.
(82) Von Puttkamer, K.; Quack, M. *Chimia* **1985**, *34*, 359.
(83) Anderson, J. B.; Andres, R. P.; Fenn, J. B. *Adv. Chem. Phys.* **1966**, *10*, 275.
(84) Smalley, R. E.; Wharton, L.; Levy, D. H. *Acc. Chem. Res.* **1977**, *10*, 139.
(85) Dyke, T. R.; Howard, B. J.; Klemperer, W. *J. Chem. Phys.* **1972**, *56*, 2442.
(86) Howard, B. J.; Dyke, T. R.; Klemperer, W. *J. Chem. Phys.* **1984**, *81*, 5417.
(87) Novick, S. W.; Davies, P. B.; Dyke, T. R.; Klemperer, W. *J. Am. Chem. Soc.* **1973**, *95*, 8547.
(88) Novick, S. E.; Davies, P. B.; Harris, S. J.; Klemperer, W. *J. Chem. Phys.* **1973**, *59*, 2273.
(89) Harris, S. J.; Novick, S. E.; Klemperer, W. *J. Chem. Phys.* **1974**, *60*, 3208.
(90) Harris, S. J.; Janda, K. C.; Novick, S. E.; Klemperer, W. *J. Chem. Phys.* **1975**, *63*, 881.
(91) Chance, K. V.; Bowen, K. H.; Winn, J. S.; Klemperer, W. *J. Chem. Phys.* **1979**, *70*, 5157.
(92) Dixon, T. A.; Joyner, C. H.; Baiocchi, F. A.; Klemperer, W. *J. Chem. Phys.* **1981**, *74*, 6539.
(93) Altman, R. S.; Marshall, M. D.; Klemperer, W. *J. Chem. Phys.* **1982**, *77*, 4344.
(94) Barton, A. E.; Henderson, T. J.; Langridge-Smith, P. R. R.; Howard, B. J. *Chem. Phys.* **1980**, *45*, 429.
(95) Barton, A. E.; Howlett, D. J. B.; Howard, B. J. *Mol. Phys.* **1980**, *41*, 619.
(96) Joyner, C. H.; Dixon, T. A.; Baiocchi, F. A.; Klemperer, W. *J. Chem. Phys.* **1981**, *74*, 6550.
(97) Baiocchi, F. A.; Dixon, T. A.; Joyner, C. H.; Klemperer, W. *J. Chem. Phys.* **1981**, *74*, 6544.
(98) Buxton, L. W.; Campbell, E. J.; Flygare, W. H. *Chem. Phys.* **1981**, *56*, 399.
(99) Soper, P. D.; Legon, A. C.; Read, W. G.; Flygare, W. H. *J. Chem. Phys.* **1982**, *76*, 292.
(100) Legon, A. C.; Soper, P. D.; Flygare, W. H. *J. Chem. Phys.* **1981**, *74*, 4944.
(101) Legon, A. C.; Soper, P. D.; Flygare, W. H. *J. Chem. Phys.* **1981**, *74*, 4936.
(102) Campbell, E. J.; Read, W. G.; Shea, J. A. *Chem. Phys. Lett.* **1983**, *94*, 69.
(103) Read, W. G.; Campbell, E. J. *J. Chem. Phys.* **1983**, *78*, 6515.
(104) Legon, A. C.; Campbell, E. J.; Flygare, W. H. *J. Chem. Phys.* **1982**, *76*, 2261.
(105) Lisy, J. M.; Tramer, A.; Vernon, M. F.; Lee, Y. T. *J. Chem. Phys.* **1981**, *75*, 4733.
(106) Gentry, W. R. *Resonances in Electron–Molecule Scattering, van der Waals Complexes and Reactive Chemical Dynamics*; Truhlar, D. G., Ed.; ACS Symposium Series 263; American Chemical Society: Washington, DC, 1984.
(107) Casassa, M. P.; Western, C. M.; Janda, K. C. *Resonances in Electron–Molecule Scattering, van der Waals Complexes and Reactive Chemical Dynamics*; Truhlar, D. G., Ed.; ACS Symposium Series 263; American Chemical Society: Washington, DC, 1984.
(108) Michael, D. W.; Lisy, J. M. *J. Chem. Phys.* **1986**, *85*, 2528.
(109) Gough, T. E.; Miller, R. E. *Chem. Phys. Lett.* **1982**, *87*, 280.
(110) Kolenbrander, K. D.; Lisy, J. M. *J. Chem. Phys.* **1986**, *85*, 6227.
(111) Gough, T. E.; Miller, R. E.; Scoles, G. *J. Chem. Phys.* **1978**, *69*, 1588.
(112) Gough, T. E.; Miller, R. E.; Scoles, G. *J. Phys. Chem.* **1981**, *85*, 4041.
(113) Miller, R. E.; Watts, R. O.; Ding, A. *Chem. Phys.* **1984**, *83*, 155.
(114) Miller, R. E.; Vohralik, P. F.; Watts, R. O. *J. Chem. Phys.* **1984**, *80*, 5453.
(115) Fischer, G.; Miller, R. E.; Vohralik, P. F.; Watts, R. O. *J. Chem. Phys.* **1985**, *83*, 147.
(116) Huang, Z. S.; Jucks, K. W.; Miller, R. E. *J. Chem. Phys.* **1986**, *85*, 6905.
(117) Huang, Z. S.; Jucks, K. W.; Miller, R. E. *J. Chem. Phys.* **1986**, *85*, 3338.
(118) Jucks, K. W.; Huang, Z. S.; Dayton, D.; Miller, R. E.; Lafferty, W. J. *J. Chem. Phys.* **1987**, *86*, 4341.
(119) Jucks, K. W.; Huang, Z. S.; Miller, R. E. *J. Chem. Phys.* **1987**, *86*, 1098.
(120) Fraser, G. T.; Pine, A. S.; Lafferty, W. J.; Miller, R. E. *J. Chem. Phys.* **1987**, *87*, 1502.
(121) Hayman, G. D.; Hodge, J.; Howard, B. J.; Muenter, J. S.; Dyke, T. R. *Chem. Phys. Lett.* **1985**, *118*, 12.
(122) Hayman, G. D.; Hodge, J.; Howard, B. J.; Muenter, J. S.; Dyke, T. R. *J. Chem. Phys.* **1987**, *87*, 1670.
(123) Hodge, J.; Hayman, G. D.; Dyke, T. R.; Howard, B. J. *J. Chem. Soc., Faraday Trans. 2* **1986**, *82*, 1137.
(124) Prichard, D.; Muenter, J. S.; Howard, B. J. *Chem. Phys. Lett.* **1987**, *135*, 9.
(125) Lovejoy, C. M.; Schuder, M. D.; Nesbitt, D. J. *Chem. Phys. Lett.* **1986**, *127*, 374.
(126) Lovejoy, C. M.; Schuder, M. D.; Nesbitt, D. J. *J. Chem. Phys.* **1986**, *85*, 4890.
(127) Lovejoy, C. M.; Nesbitt, D. J. *Rev. Sci. Instrum.* **1987**, *58*, 807.
(128) Lovejoy, C. M.; Nesbitt, D. J. *J. Chem. Phys.* **1987**, *86*, 3151.
(129) Lovejoy, C. M.; Schuder, M. D.; Nesbitt, D. J. *J. Chem. Phys.* **1987**, *86*, 5337.
(130) Lovejoy, C. M.; Nesbitt, D. J. *J. Chem. Phys.* **1987**, *87*, 1450.

(131) Amirav, A. A.; Even, U.; Jortner, J. *Chem. Phys. Lett.* **1981**, *83*, 1.
(132) Hopkins, G. A.; Maroncelli, M.; Nibler, J. W.; Dyke, T. R. *Chem. Phys. Lett.* **1985**, *114*, 97.
(133) Maroncelli, M.; Hopkins, G. A.; Nibler, J. W.; Dyke, T. R. *J. Chem. Phys.* **1985**, *83*, 2129.
(134) Pubanz, G. A.; Maroncelli, M.; Nibler, J. W. *Chem. Phys. Lett.* **1985**, *120*, 313.
(135) Marshall, M. D.; Charo, A.; Leung, H. O.; Klemperer, W. *J. Chem. Phys.* **1985**, *83*, 4924.
(136) Fraser, G. T.; Nelson, D. D., Jr.; Charo, A.; Klemperer, W. *J. Chem. Phys.* **1985**, *82*, 2535.
(137) Nelson, D. D., Jr.; Fraser, G. T.; Klemperer, W. *Science (Washington, D.C.)*, in press.
(138) Nelson, D. D., Jr.; Klemperer, W.; Fraser, G. T.; Lovas, F. J.; Suenram, R. D. *J. Chem. Phys.*, in press.
(139) Robinson, R. L.; Gwo, D.-H.; Ray, D.; Saykally, R. J. *J. Chem. Phys.* **1987**, *86*, 5211.
(140) Robinson, R. L.; Ray, D.; Gwo, D.-H.; Saykally, R. J. *J. Chem. Phys.* **1987**, *87*, 5149.
(141) Robinson, R. L.; Gwo, D.-H.; Saykally, R. J. *J. Chem. Phys.* **1987**, *87*, 5211.
(142) DeLeon, R. L.; Meunter, J. S. *J. Chem. Phys.* **1984**, *80*, 6092.
(143) Busarow, K. L.; Blake, G. A.; Laughlin, K. B.; Cohen, R. C.; Yee, Y. T.; Saykally, R. J. *Chem. Phys. Lett.* **1987**, *141*, 289.
(144) Kuipers, G. A. *J. Mol. Spectrosc.* **1958**, *2*, 75.
(145) Smith, D. F. *J. Chem. Phys.* **1958**, *28*, 1040.
(146) Smith, D. F. *J. Mol. Spectrosc.* **1959**, *3*, 473.
(147) Herget, W. F.; Gailar, N. M.; Lovell, R. J.; Nielsen, A. H. *J. Opt. Soc. Am.* **1960**, *50*, 1264.
(148) Himes, J. L.; Wiggins, T. A. *J. Mol. Spectrosc.* **1971**, *40*, 418.
(149) Reddington, R. L. *J. Phys. Chem.* **1982**, *86*, 552.
(150) Andrews, L.; Johnson, G. L. *Chem. Phys. Lett.* **1983**, *96*, 133.
(151) Holmgren, S. L.; Waldman, M.; Klemperer, W. *J. Chem. Phys.* **1977**, *67*, 4414.
(152) Hutson, J. M.; Howard, B. J. *Mol. Phys.* **1980**, *41*, 1123.
(153) Barton, A. E.; Howard, B. J. *Faraday Discuss. Chem. Soc.* **1982**, *73*, 45.
(154) Yarkony, D. R.; O'Neil, S. V.; Schaefer, H. F., III; Baskin, C. P.; Bender, C. F. *J. Chem. Phys.* **1974**, *60*, 855.
(155) Curtiss, L. A.; Pople, J. A. *J. Mol. Spectrosc.* **1976**, *61*, 1.
(156) Klein, M. L.; McDonald, I. R.; O'Shea, S. F. *J. Chem. Phys.* **1978**, *69*, 63.
(157) Michael, D. W.; Dykstra, C. E.; Lisy, J. M. *J. Chem. Phys.* **1984**, *81*, 5998.
(158) Klemperer, W. *Ber. Bunsenges. Phys. Chem.* **1974**, *78*, 128.
(159) Larvor, M.; Houdeau, J.-P.; Haeusler, C. *Can. J. Phys.* **1978**, *56*, 334.
(160) Lovejoy, C. M.; Nesbitt, D. J., private communication.
(161) Sakai, K.; Kiode, A.; Kihara, T. *Chem. Phys. Lett.* **1977**, *47*, 416.
(162) Bryant, G. W.; Eggers, D. F.; Watts, R. O., private communication.
(163) Barton, A. E.; Chablo, A.; Howard, B. J. *Chem. Phys. Lett.* **1979**, *60*, 414.
(164) Kopec, R. L. Ph.D. Thesis, Indiana University, Bloomington, IN, 1981.
(165) Lobue, J. M.; Rice, J. K.; Novick, S. E. *Chem. Phys. Lett.* **1984**, *112*, 376.
(166) Miller, R. E.; Watts, R. O. *Chem. Phys. Lett.* **1984**, *105*, 409.
(167) Huang, Z. S.; Miller, R. E., private communication.
(168) Dulmage, W. J.; Lipscomb, W. N. *Acta Crystallogr.* **1951**, *4*, 330.
(169) Kofranck, M.; Karpfen, A. Lischka, H. *Chem. Phys.* **1987**, *113*, 53.
(170) Lieb, S. G.; Bevan, J. W. *Chem. Pphys. Lett.* **1985**, *122*, 284.
(171) Jucks, K. W.; Miller, R. E., private communication.
(172) Sagarik, K.; Ahlrichs, R.; Brode, S. *Mol. Phys.* **1986**, *57*, 1247.
(173) Liu, S.-Y.; Dykstra, C. E.; Kolenbrander, K.; Lisy, J. *J. Chem. Phys.* **1986**, *85*, 2077.
(174) Frisch, M. J.; Del Bene, J. E.; Binkley, J. S.; Schaefer, H. F., III. *J. Chem. Phys.* **1986**, *84*, 2279.
(175) Latajka, Z.; Scheiner, S. *J. Chem. Phys.* **1986**, *84*, 341.
(176) LeRoy, R. J.; Van Kranendonk, J. *J. Chem. Phys.* **1974**, *61*, 4750.
(177) Hutson, J. M.; LeRoy, R. J. *J. Chem. Phys.* **1985**, *83*, 1197.
(178) Hutson, J. M. *J. Chem. Soc., Faraday Trans. 2* **1986**, *82*, 1163.
(179) LeRoy, R. J.; Carley, J. S. *Adv. Chem. Phys.* **1980**, *42*, 353.
(180) Ewing, G. E. *J. Chem. Phys.* **1980**, *72*, 2096.
(181) LeRoy, R. J.; Hutson, J. M. *J. Chem. Phys.* **1986**, *86*, 837.
(182) Waaijer, M.; Reuss, J. *Chem. Phys.* **1981**, *63*, 263.
(183) Buck, U. *Faraday Discuss. Chem. Soc.* **1982**, *73*, 187.
(184) Buck, U.; Meyer, H.; LeRoy, R. J. *J. Chem. Phys.* **1984**, *80*, 5589.
(185) Bernholdt, D. E.; Liu, S.-Y.; Dykstra, C. E. *J. Chem. Phys.* **1986**, *85*, 5120.
(186) Lovejoy, C. M.; Nelson, D. D., Jr.; Nesbitt, D. J. *J. Chem. Phys.* **1987**, *87*, 5621.
(187) Jucks, K. W.; Miller, R. E. *J. Chem. Phys.* **1987**, *87*, 5629.
(188) Watson, J. K. G. *Vibrational Spectra and Structure*; Durig, J. R., Ed.; Elsevier: New York, 1977.
(189) Lovejoy, C. M.; Nesbitt, D. J., private communication.
(190) Neilson, W. B.; Gordon, R. G. *J. Chem. Phys.* **1973**, *58*, 4149.
(191) Hutson, J. M.; Howard, B. J. *Mol. Phys.* **1981**, *43*, 493.
(192) Hutson, J. M.; Howard, B. J. *Mol. Phys.* **1982**, *45*, 769.
(193) Hutson, J. M.; Howard, B. J. *Mol. Phys.* **1982**, *45*, 791.
(194) Douketis, C.; Hutson, J. M.; Orr, B. J.; Scoles, G. *Mol. Phys.* **1984**, *52*, 763.
(195) Hutson, J. M. *J. Chem. Phys.* **1984**, *81*, 2357.
(196) Liu, S.-Y.; Dykstra, C. E. *J. Phys. Chem.* **1986**, *90*, 3097.
(197) Liu, S.-Y.; Dykstra, C. E. *Chem. Phys. Lett.* **1987**, *136*, 22.
(198) Gutowsky, H. S.; Klots, T. D.; Chuang, C.; Schmuttenmaer, C. A.; Emilsson, T. *J. Chem. Phys.* **1987**, *86*, 569.
(199) Gutowsky, H. S.; Klots, T. D.; Chuang, C. Keen, J. D.; Schmuttenmaer, C. A.; Emilsson, T. E. *J. Am. Chem. Soc.* **1985**, *107*, 7174.
(200) Turrell, G. C.; Vu, H.; Vodar, B. *J. Chem. Phys.* **1960**, *33*, 315.
(201) Lovejoy, C. M.; Nesbitt, D. J. *Chem. Phys. Lett.*, submitted.
(202) Benzel, M. A.; Dykstra, C. E. *J. Chem. Phys.* **1983**, *78*, 4052.
(203) Lindeman, T.; Lovejoy, C. M.; Nesbitt, D. J., private communication.
(204) Liu, S.-Y.; Dykstra, C. E.; Malik, D. J. *Chem. Phys. Lett.* **1986**, *130*, 403.
(205) Hurst, G. J. B.; Fowler, P. W.; Stove, A. J.; Buckingham, A. D. *Int. J. Quant. Chem.* **1986**, *29*, 1223.
(206) Sapse, A.-M. *J. Chem. Phys.* **1983**, *78*, 5738.
(207) Kukolich, S. G.; Bumgarner, R. E.; Pauley, D. J. *Chem. Phys. Lett.* **1987**, *141*, 12.
(208) Spackman, M. A., private communication.
(209) Dayton, D. C.; Miller, R. E., private communication.
(210) Botschwina, P., private communication.
(211) Jucks, K. W.; Miller, R. E. *J. Chem. Phys.* **1987**, *86*, 6637.
(212) Wilson, E. B., Jr.; Decius, J. C.; Cross, P. C. *Molecular Vibrations*; Dover: New York, 1955.
(213) Nelson, D. D.; Fraser, G. T.; Klemperer, W. *J. Chem. Phys.* **1985**, *82*, 4483.
(214) Read, W. G.; Flygare, W. H. *J. Chem. Phys.* **1982**, *76*, 2238.
(215) Huang, Z. S.; Miller, R. E., private communication.
(216) Shea, J. A.; Flygare, W. R. *J. Chem. Phys.* **1987**, *76*, 4857.
(217) Huang, Z. S.; Miller, R. E., private communication.
(218) Jucks, K. W.; Miller, R. E. *Chem. Phys. Lett.* **1987**, *139*, 201.
(219) Thomas, R. K. *Proc. R. Soc. London, Ser. A* **1971**, *325*, 133.
(220) Curtiss, L. A.; Pople, J. A. *J. Mol. Spectrosc.* **1973**, *48*, 413.
(221) Hoffbauer, M. A.; Giese, C. F.; Gentry, W. R. *J. Chem. Phys.* **1983**, *79*, 192.
(222) Ebenstein, W. L.; Muenter, J. S. *J. Chem. Phys.* **1984**, *80*, 3989. DeLeon, R. L.; Muenter, J. S. *J. Chem. Phys.* **1984**, *80*, 3992.
(223) Lovas, F. J.; Suenram, R. D. *J. Chem. Phys.*, in press.
(224) Joyner, C. H.; Dixon, T. A.; Baiocchi, F. A.; Klemperer, W. *J. Chem. Phys.* **1981**, *75*, 5285.
(225) Weisskopf, V.; Wigner, E. *Z. Phys.* **1930**, *63*, 54.
(226) Casassa, M. P.; Woodward, A. M.; Stephenson, J. C.; King, D. S. *J. Chem. Phys.* **1986**, *85*, 6235.
(227) Ewing, G. E. *J. Chem. Phys.* **1979**, *71*, 3143.
(228) Gentry, W. R. In *Resonances in Electron–Molecule Scattering, van der Waals Complexes and Reactive Chemical Dynamics*; Truhlar, D. J., Ed.; ACS Symposium Series 263; American Chemical Society: Washington, DC, 1984.
(229) Hutson, J. M. *J. Chem. Phys.* **1984**, *81*, 2357.
(230) Buckingham, A. D.; Fowler, P. W. *J. Chem. Phys.* **1983**, *79*, 6426.
(231) Baiocchi, F. A.; Reiker, W.; Klemperer, W. *J. Chem. Phys.* **1983**, *79*, 6428.
(232) Nesbitt, D. J. *Structure of Small Molecules and Ions*; Naaman, R., Ed.; Plenum: New York, in press.